Published for SISSA by Springer

Received: *September 30, 2025*
Accepted: *March 14, 2026*
Published: *May 15, 2026*

Measurement of the dineutrino system kinematic variables in dileptonic top quark pair production in proton-proton collisions at $\sqrt{s} = 13$ TeV

The CMS collaboration

Full author list at the end of the paper

E-mail: cms-publication-committee-chair@cern.ch

Abstract: Differential top quark pair production cross sections are measured in the dilepton final states e^+e^-, $\mu^+\mu^-$, and $e^\pm\mu^\mp$, as a function of kinematic variables of the two-neutrino system: the transverse momentum $p_T^{\nu\nu}$ of the dineutrino system, the minimum distance in azimuthal angle between $\vec{p}_T^{\,\nu\nu}$ and leptons, and in two dimensions in bins of both observables. The measurements are performed using CERN LHC proton-proton collisions at $\sqrt{s} = 13$ TeV, recorded by the CMS detector between 2016 and 2018, corresponding to an integrated luminosity of 138 fb^{-1}. The measured cross sections are unfolded to the particle level using an unregularized least squares method. Results are compared with predictions by the standard model of particle physics, and found to be in agreement with theoretical calculations as well as Monte Carlo simulations.

Keywords: Hadron-Hadron Scattering, Particle and Resonance Production, Top Physics

ArXiv ePrint: 2510.00160

https://doi.org/10.1007/JHEP05(2026)175

Contents

1 Introduction

Precision measurements of the top quark pair ($\mathrm{t\bar{t}}$) production cross section provide stringent tests for the validity of the standard model of particle physics (SM) while playing a crucial role in the search for new phenomena. The large $\mathrm{t\bar{t}}$ data samples collected at the CERN LHC have made several measurements of differential cross sections possible in various $\mathrm{t\bar{t}}$ decay channels and at different center-of-mass energies [1–23]. All measurements to date were performed as functions of observables that characterize the kinematic properties of either the visible part of the event, such as jets or charged leptons, or intermediate particles, such as the top (anti)quark or the W boson. However, there are beyond-the-SM (BSM) physics scenarios that mostly modify the invisible part of the signature. Precise measurements of undetected particles in the event, can therefore reveal signs of new phenomena.

This paper presents the first measurements of the differential $\mathrm{t\bar{t}}$ cross section as a function of the transverse momentum of the dineutrino system, $p_{\mathrm{T}}^{\nu\nu}$, and the minimum azimuthal distance between $\vec{p}_{\mathrm{T}}^{\,\nu\nu}$ and the transverse momentum of a charged lepton, $\min[\Delta\phi(\vec{p}_{\mathrm{T}}^{\,\nu\nu}, \vec{p}_{\mathrm{T}}^{\,\ell})]$, which can be precisely reconstructed in dileptonic final states. In addition, a two-dimensional (2D) measurement as a function of both observables is performed. For the SM $\mathrm{t\bar{t}}$ production process, neutrinos from the leptonic decays of the W boson account for most of the missing transverse momentum $\vec{p}_{\mathrm{T}}^{\,\mathrm{miss}}$ of the event, while for BSM processes, contributions to $\vec{p}_{\mathrm{T}}^{\,\mathrm{miss}}$ from undetected particles are also present in the event. These additional contributions can weaken the angular correlation between $\vec{p}_{\mathrm{T}}^{\,\nu\nu}$ and the lepton direction, leading to a broader $\min[\Delta\phi(\vec{p}_{\mathrm{T}}^{\,\nu\nu}, \vec{p}_{\mathrm{T}}^{\,\ell})]$ distribution. The selection of the two observables for the cross section measurements in this analysis is, therefore, targeted to validate the modelling of the SM $\mathrm{t\bar{t}}$ process in a phase space sensitive to BSM scenarios that exhibit a comparable signature but include additional sources of undetected particles.

JHEP05(2026)175

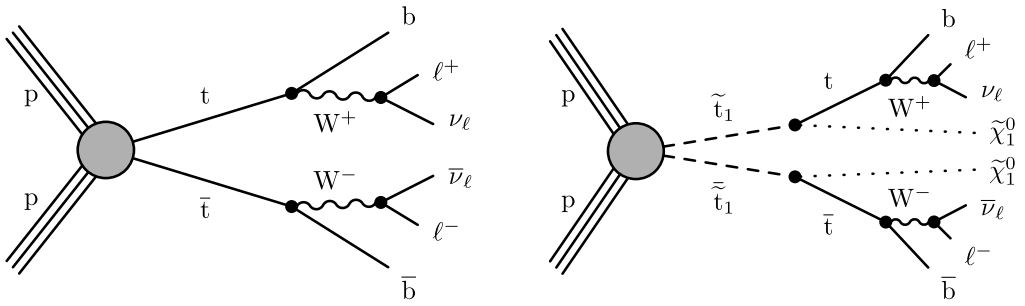

Figure 1. In the left diagram, the SM $t\bar{t}$ production process is sketched, whereas the right diagram shows the production of a hypothetical top squark pair, $\tilde{t}_1\bar{\tilde{t}}_1$, with both top squarks decaying to a top quark and a neutralino, $\tilde{\chi}_1^0$. This analysis focuses on signatures, where both of the W bosons decay leptonically.

Squarks are superpartners of quarks as predicted by supersymmetry [24]. In figure 1, a diagram of $t\bar{t}$ production in the dilepton final state is compared to that of a top squark pair production, as an example of a BSM process [25]. The presence of neutralinos, that neither decay to SM particles nor are detectable within the detector, modifies the kinematic properties of the invisible part of the BSM event that otherwise exhibits a final state identical to that of the $t\bar{t}$ decay. Dedicated searches for top squark pair production in the dilepton final state found significant contributions of $t\bar{t}$ events in the search phase space [26–28].

A precise measurement of the dineutrino system in dileptonic $t\bar{t}$ events requires a good resolution of $\vec{p}_{\mathrm{T}}^{\,\mathrm{miss}}$, which serves as a proxy for the transverse momentum of the dineutrino system. The magnitude and direction of $\vec{p}_{\mathrm{T}}^{\,\mathrm{miss}}$ are evaluated from the negative $\vec{p}_{\mathrm{T}}$ sum of all reconstructed objects in an event, exploiting momentum conservation. The $\vec{p}_{\mathrm{T}}^{\,\mathrm{miss}}$ resolution is affected by mismeasurements of other particles that can happen due to detector effects and/or as a result of additional proton-proton (pp) collisions in the same or adjacent bunch crossing (pileup). A dedicated correction based on a regression using machine learning methods is developed to improve the $\vec{p}_{\mathrm{T}}^{\,\mathrm{miss}}$ resolution.

Absolute and normalized differential cross sections are measured in the dilepton final states e^+e^-, $\mu^+\mu^-$, and $e^\pm\mu^\mp$, derived for a fiducial phase space close to the acceptance of the detector and extracted by an unregularized unfolding using a least squares minimization. The results are compared to predictions from Monte Carlo (MC) event generators at the matrix element (ME) level with next-to-leading order (NLO) accuracy in quantum chromodynamics (QCD), which are interfaced with a parton shower (PS) simulation. In addition, the results are compared to fixed-order predictions at NLO and next-to-NLO (NNLO) precision [29].

The paper is structured as follows: Section 2 briefly describes the main features of the CMS detector. In section 3, the recorded data samples are briefly introduced and settings for MC simulation of signal and background processes are detailed. Section 4 presents the object reconstruction and the event selection, followed by the description of the correction of $\vec{p}_{\mathrm{T}}^{\,\mathrm{miss}}$ in section 5. The systematic uncertainties and the results, including comparisons to different predictions, are discussed in sections 6 and 7, respectively. Finally, the analysis is summarised in section 8. Tabulated results can be found in a HEPData record [30].

JHEP05(2026)175

2 The CMS detector

The CMS apparatus [31, 32] is a multipurpose, nearly hermetic detector, designed to trigger on [33–35] and identify electrons, muons, photons, charged and neutral hadrons [36–38]. Its central feature is a superconducting solenoid of 6 m internal diameter, providing a magnetic field of 3.8 T. Within the solenoid volume are a silicon pixel and strip tracker, a lead tungstate crystal electromagnetic calorimeter (ECAL), and a brass and scintillator hadron calorimeter (HCAL), each composed of a barrel and two endcap sections. Forward calorimeters extend the pseudorapidity (η) coverage provided by the barrel and endcap detectors. Muons are reconstructed using gas-ionization detectors embedded in the steel flux-return yoke outside the solenoid. Events of interest are selected using a two-tiered trigger system. The first level, composed of custom hardware processors, uses information from the calorimeters and muon detectors to select events at a rate of around 100 kHz within a fixed latency of 4 μs [33]. The second level, known as the high-level trigger, consists of a farm of processors running a version of the full event reconstruction software optimized for fast processing, and reduces the event rate to around 1 kHz before data storage [34].

More detailed descriptions of the CMS detector, together with a definition of the coordinate system used and the relevant kinematic variables, can be found in refs. [31, 32].

3 Data and simulated samples

The measurements presented in this paper are based on pp collision data recorded between 2016 and 2018 at a center-of-mass energy of 13 TeV, corresponding to an integrated luminosity of 138 fb^{-1} [39–41] with 36.3, 41.5, and 59.8 fb^{-1} of data recorded in 2016, 2017, and 2018, respectively.

Both the signal and the SM background processes are simulated using MC event generators. Simulated samples are produced separately for each data-taking period to match the corresponding pileup and detector conditions. All simulated samples use parton distribution functions (PDFs) as implemented in NNPDF3.1 [42, 43] at NNLO accuracy in perturbative QCD. All ME event generators are interfaced with PYTHIA v8.230 [44] for the simulation of the parton showering and hadronization using the CP5 tune [45] unless stated otherwise in the text. The detector response is simulated with GEANT4 [46].

The $\mathrm{t\bar{t}}$ production process is simulated using the POWHEG v2 [47–49] event generator at NLO precision in QCD with the top quark mass set to 172.5 GeV. Top quark pairs in which both W bosons decay into either an electron or muon belong to the signal sample and are referred to as "$\mathrm{t\bar{t}}$ ($\ell\ell$)" and/or "dileptonic $\mathrm{t\bar{t}}$" in the following. All other decay channels, including the production of one or more tau leptons, are denoted as "$\mathrm{t\bar{t}}$ other". Additional $\mathrm{t\bar{t}}$ samples using the same event generator are produced with modified parameters for the underlying event tune, color reconnection scheme, jet matching scheme, and top quark mass, and are used in the estimation of the impact of theoretical uncertainties. A $\mathrm{t\bar{t}}$ sample generated with MADGRAPH5_aMC@NLO v2.4.2 (MG5) [50] at NLO accuracy and interfaced with PYTHIA through the FxFx [51] matching and merging scheme is used for the determination of corrections that improve the experimental $\vec{p}_{\mathrm{T}}^{\,\mathrm{miss}}$ resolution detailed in section 5. This sample is referred to as MC@NLO+PYTHIA in the following. Another

JHEP05(2026)175

alternative $t\bar{t}$ sample is generated with the POWHEG v2 generator interfaced with HERWIG v7.1 [52] using the CH3 tune [53], and is referred to as POWHEG+HERWIG.

Background processes are modelled using different MC event generators. Drell-Yan events with additional jets and two leptons in the final state (DY+jets) are produced at NLO using MG5. Events are passed through PS and hadronization using the FxFx merging scheme.

The same event generator is used for the production of a W boson that subsequently decays to a lepton and neutrino. Events contain up to four additional jets, modelled at leading order in perturbative QCD, and matched to jets produced during PS and hadronization with the MLM scheme [54]. The electroweak top quark productions, referred to as "single top" hereafter, are modelled at NLO accuracy using POWHEG v2 [55] for the tW process and the t-channel production, and using MG5 in the case of the s-channel production. For the tW process, the description based on the diagram subtraction (DS) scheme is applied [56] in order to handle the overlap and interference with $t\bar{t}$ production. Another tW sample based on the diagram removal (DR) scheme [56] is used for the estimation of theoretical uncertainties.

The production of $t\bar{t}$ in association with a W or Z boson ($t\bar{t}W/Z$) is modeled at NLO accuracy using MG5. Diboson production processes, including WW, WZ, and ZZ, are generated at leading order using PYTHIA. The contribution of QCD multijet production in the analysis phase-space is negligible.

The expected yield of $t\bar{t}$ events is determined using a cross section calculated with the TOP++ [57] program at NNLO plus next-to-next-to-leading-logarithmic accuracy [58–61], assuming a top quark mass of 172.5 GeV. The simulated p_T spectra of top quarks are reweighted to NNLO cross sections using NNLO/NLO K-factors [62]. Yields from the W+jets and high-mass DY+jets processes are calculated using NNLO accuracy cross sections [63, 64], while the yield of low-mass DY+jets and the $t\bar{t}W/Z$ processes are calculated using NLO accuracy cross sections from the MG5 generator. A cross section calculation at approximate NNLO is used for the single top tW [65] process, while yields from the single top s- and t-channel processes are determined using NLO cross sections [66, 67]. Cross sections calculated at NNLO accuracy [68] are used to determine the WW yield, whereas NLO cross sections [69] are applied to determine the WZ and ZZ diboson process yields.

4 Object reconstruction and event selection

Events passing dilepton and single-lepton triggers are used for the offline analysis. The trigger criteria vary by data-taking period. For dielectron and electron-muon triggers, the transverse momentum p_T of the (sub)leading lepton is required to pass a threshold of 23 (12) GeV. The maximum p_T threshold on the (sub)leading muon in dimuon triggers is 17 (8) GeV. The threshold on the lepton p_T is 27 (32) GeV in 2016 (2017–2018) for single electron triggers, and 24 (27) GeV in 2016/2018 (2017) for single muon triggers.

The primary vertex (PV) is taken to be the vertex corresponding to the hardest scattering in the event, evaluated using tracking information alone, as described in section 9.4.1 of ref. [70]. The particle-flow (PF) algorithm [71] aims to reconstruct and identify each individual particle in the event, with an optimized combination of information from various elements of the CMS detector. The energy of photons is obtained from the ECAL measurement. The energy of electrons is determined from a combination of the electron momentum at the PV,

JHEP05(2026)175

the energy of the corresponding ECAL cluster, and the energy sum of all bremsstrahlung photons spatially compatible with originating from the electron track. The energy of muons is obtained from the curvature of the corresponding track. The energy of charged hadrons is determined from a combination of their momenta measured in the tracker and the matching ECAL and HCAL energy deposits, corrected for the response function of the calorimeters to hadronic showers. Finally, the energy of neutral hadrons is obtained from the corresponding corrected ECAL and HCAL energies.

Electron candidates are vetoed if their associated ECAL cluster is reconstructed within the transition region of the ECAL, which corresponds to the η range of $1.44 < |\eta| < 1.57$. Misidentified and nonprompt electrons are further suppressed by implementing selections based on discriminating quantities, such as shower shape variables, relative isolation, longitudinal and transverse impact parameters with respect to the PV, and photon conversion veto observables. For electrons, the relative isolation is defined as the p_{T} sum of all neutral and charged hadrons, and photon candidates within an angular distance $\Delta R = \sqrt{(\Delta\phi)^2 + (\Delta\eta)^2}$ of 0.3 from the electron in the η–ϕ space, divided by the p_{T} of the electron candidate. Depending on the p_{T} and η of the electron candidate, a maximum relative isolation in the range 0.05–0.1 is enforced. Muon candidates are required to have matching tracks in the inner tracker and the muon system, with track quality criteria, relative isolation, and impact parameter requirements suppressing nonprompt or misidentified muons. For muons, the relative isolation is based on contributions within a distance of 0.4 from the muon candidate, applying a maximal relative isolation of 0.15. For both electrons and muons, the relative isolation is corrected for pileup effects by removing charged PF candidates associated with pileup vertices, and by estimating the contribution of neutral particles from pileup to be subtracted from the p_{T} sum [72, 73].

Jets are clustered using the anti-k_{T} algorithm [74, 75] with a distance parameter of 0.4. Jets within an angular distance $\Delta R < 0.4$ of selected leptons are not considered in further steps of the analysis. To reduce contributions from jets originating from pileup vertices, additional requirements for jets reconstructed with $p_{\mathrm{T}} < 50\,\mathrm{GeV}$ are applied [76]. Jets originating from the hadronization of b quarks are identified with the DeepJet algorithm [77], using a working point corresponding to an efficiency of up to 92% for b quark jets and a misidentification rate of 10 (40–50)% for jets originating from light-flavor quarks and gluons (c quarks).

The missing transverse momentum vector $\vec{p}_{\mathrm{T}}^{\,\mathrm{miss}}$ is computed as the negative vector sum of the transverse momenta of all the PF candidates in an event, and its magnitude is denoted as $p_{\mathrm{T}}^{\mathrm{miss}}$ [78]. The $\vec{p}_{\mathrm{T}}^{\,\mathrm{miss}}$ is modified to account for corrections to the energy scale of the reconstructed jets in the event and denoted as $\vec{p}_{\mathrm{T,PF}}^{\,\mathrm{miss}}$. The pileup-per-particle identification (PUPPI) algorithm [79] is applied to reduce the pileup dependence of the $\vec{p}_{\mathrm{T}}^{\,\mathrm{miss}}$ observable. For each PF candidate, a weight is computed based on the probability to originate from the PV. For charged particles, the assignment of the weight is based on the track-vertex association. For neutral PF candidates, instead, the weight computation is based on the p_{T} of the surrounding particles, as described in ref. [78]. The $\vec{p}_{\mathrm{T}}^{\,\mathrm{miss}}$ computed from the PF candidates weighted by their probability to originate from the PV is denoted as $\vec{p}_{\mathrm{T,PUPPI}}^{\,\mathrm{miss}}$. Further corrections to $\vec{p}_{\mathrm{T,PUPPI}}^{\,\mathrm{miss}}$ are derived in this analysis using a deep neural network (DNN) in order to improve the $p_{\mathrm{T}}^{\mathrm{miss}}$ resolution in dileptonic $\mathrm{t\bar{t}}$ events, especially at high values of

JHEP05(2026)175

$p_{\mathrm{T}}^{\mathrm{miss}}$. This procedure is further detailed in section 5 and the corrected $\vec{p}_{\mathrm{T}}^{\mathrm{miss}}$ is denoted as $\vec{p}_{\mathrm{T,DNN}}^{\mathrm{miss}}$. Anomalous high-$p_{\mathrm{T}}^{\mathrm{miss}}$ events can occur due to a variety of failures in the object reconstruction, detector malfunctions, and/or noncollision backgrounds. Such events are rejected by event filters designed to identify more than 85–90% of the spurious high-$p_{\mathrm{T}}^{\mathrm{miss}}$ events with a misidentification rate of less than 0.1% [78].

The event selection closely follows that of ref. [18] with the exception that the requirement on missing transverse momentum is applied to $\vec{p}_{\mathrm{T,DNN}}^{\mathrm{miss}}$ rather than $\vec{p}_{\mathrm{T,PF}}^{\mathrm{miss}}$. Events with two oppositely charged leptons that fulfill $|\eta| < 2.4$ and $p_{\mathrm{T}} > 25$ (20) GeV for the leading (subleading) lepton are selected and split into the same-flavor $\mathrm{e^+e^-}/\mu^+\mu^-$ and the different-flavor $\mathrm{e}^{\pm}\mu^{\mp}$ channels. Events containing additional leptons (electrons or muons) with $p_{\mathrm{T}} > 15$ GeV are rejected. Contributions from low-mass resonances decaying to two leptons are suppressed by requiring a minimal invariant mass $m_{\ell\ell}$ of the two leptons of 20 GeV. In order to reduce the contribution from DY+jet events, the events in the same-flavor channels are required to fulfill $p_{\mathrm{T,DNN}}^{\mathrm{miss}} > 40$ GeV and are vetoed if $m_{\ell\ell}$ is compatible with the Z boson mass [80] within 15 GeV. Selected events must contain at least two reconstructed jets with $p_{\mathrm{T}} > 30$ GeV and $|\eta| < 2.4$, of which at least one is b tagged [81].

The numbers of expected events from simulation and of observed events in data are shown in table 1. The signal process $\mathrm{t\bar{t}}$ ($\ell\ell$) comprises 78% of the selected events. The largest background contribution arises from other $\mathrm{t\bar{t}}$ processes, contributing to 13% of the selected sample. It mostly contains events where at least one W boson decays to a τ lepton. The next background contributions in size are single top and DY processes, with 4.2 and 4.0% contributions to the selected samples, respectively. Distributions of a selected set of kinematic observables are shown in figure 2. The simulated samples reproduce the distributions in data well.

5 Improving the $p_{\mathrm{T}}^{\mathrm{miss}}$ resolution for dileptonic $\mathrm{t\bar{t}}$ events

Since the $\vec{p}_{\mathrm{T}}^{\mathrm{miss}}$ is used as a measure of the $\vec{p}_{\mathrm{T}}$ of the two prompt neutrinos ($\vec{p}_{\mathrm{T}}^{\,\nu\nu}$) produced in dileptonic $\mathrm{t\bar{t}}$ decays, it is important to ensure an accurate reconstruction of its magnitude and direction. Poor resolution or large biases of the reconstructed $\vec{p}_{\mathrm{T}}^{\mathrm{miss}}$, denoted as $\vec{p}_{\mathrm{T,rec.}}^{\mathrm{miss}}$, can compromise the stability of the unfolding process and lead to a reduced number of bins for the final measurements. Other than those coming from the two neutrinos from top quark decays, there are two additional sources that contribute to the evaluation of $\vec{p}_{\mathrm{T}}^{\mathrm{miss}}$ in dileptonic $\mathrm{t\bar{t}}$ events. The first source corresponds to the production of nonprompt neutrinos from semileptonic hadron decays in jets, especially in jets originating from b quarks. These nonprompt neutrinos lead to genuine $\vec{p}_{\mathrm{T}}^{\mathrm{miss}}$ and are therefore included in the calculation of the generated $p_{\mathrm{T}}^{\mathrm{miss}}$ of an event. This quantity, defined as the magnitude of the vector sum of all simulated neutrino $\vec{p}_{\mathrm{T}}$ is denoted as $\vec{p}_{\mathrm{T,gen.}}^{\mathrm{miss}}$. The second source is the mismeasurement of particle momenta during reconstruction, with the largest impact arising from the mismeasurements in jets. A regression based on a DNN, targeting $\vec{p}_{\mathrm{T,gen.}}^{\mathrm{miss}}$, is derived to correct for the mismeasurements. The method, detailed in the following, corrects for reconstruction effects based on the targeted final state, while being independent of the exact particle kinematic properties and the description of hadronization.

JHEP05(2026)175

Process	Yields / 10^3			
	e^+e^-	$\mu^+\mu^-$	$e^\pm\mu^\mp$	All
$t\bar{t}$ ($\ell\ell$)	116 (75.2%)	221 (74.1%)	531 (80.2%)	867 (77.9%)
$t\bar{t}$ other	18.2 (11.8%)	38.6 (12.9%)	90.5 (13.7%)	147 (13.2%)
Single top	6.15 (4.0%)	11.7 (3.9%)	28.4 (4.3%)	46.3 (4.2%)
DY+jets	12.6 (8.2%)	24.8 (8.3%)	6.87 (1.0%)	44.2 (4.0%)
Diboson	0.70 (0.5%)	1.24 (0.4%)	2.43 (0.4%)	4.36 (0.4%)
$t\bar{t}$W/Z	0.49 (0.3%)	0.89 (0.3%)	1.82 (0.3%)	3.20 (0.3%)
W+jets	0.08 (0.0%)	0.08 (0.0%)	0.88 (0.1%)	1.03 (0.1%)
Sum MC	154 ± 10	298 ± 14	662 ± 27	1114 ± 47
Data	151.568	302.168	649.504	1103.240

Table 1. Data and MC simulation yields after the event selection, combined for all data-taking periods and split by channels. The uncertainties on the expected yields include systematic and statistical uncertainties (discussed in section 6). The relative contribution in percent of each process to the total expected yield of a channel is given in parentheses.

A feed-forward, fully-connected DNN with two output nodes is constructed and trained using the TensorFlow [82] backend with a keras [83] interface. The DNN architecture consists of two hidden layers with 512 and 256 nodes for the first and second layers, respectively. In order to simultaneously correct the direction and magnitude of $\vec{p}_{\mathrm{T}}^{\,\mathrm{miss}}$, the two output nodes of the DNN are the x and y components of the difference between $\vec{p}_{\mathrm{T,PUPPI}}^{\,\mathrm{miss}}$ and $\vec{p}_{\mathrm{T,gen.}}^{\,\mathrm{miss}}$. The output of the DNN is then used to correct the $\vec{p}_{\mathrm{T,PUPPI}}^{\,\mathrm{miss}}$. The network is trained based on the alternative MC@NLO+PYTHIA $t\bar{t}$ sample, which is statistically independent of the POWHEG+PYTHIA sample used in the unfolding procedure. The training is performed on dileptonic $t\bar{t}$ events passing the selection detailed in section 4, but omitting the requirement on $p_{\mathrm{T,DNN}}^{\mathrm{miss}}$. The training sample is reweighted so that the $p_{\mathrm{T,gen.}}^{\mathrm{miss}}$ distribution is uniform up to 500 GeV, and a constant weight is applied to events above 500 GeV. This allows the DNN to perform on a wider $\vec{p}_{\mathrm{T,gen.}}^{\,\mathrm{miss}}$ range rather than being biased to a specific range with the largest population in the nominal training sample. To account for varying data-taking conditions, the training is performed separately for each data-taking period, based on a total of approximately 5 million events.

The DNN is based on 17 input observables, including the x and y components of $\vec{p}_{\mathrm{T,PUPPI}}^{\,\mathrm{miss}}$, $\vec{p}_{\mathrm{T,PF}}^{\,\mathrm{miss}}$, the $\vec{p}_{\mathrm{T}}$ sum of all jets, the $\vec{p}_{\mathrm{T}}$ of the leading and subleading jets, and the $\vec{p}_{\mathrm{T}}$ of the leading lepton. Additional inputs include the invariant mass of the two leptons and all jets, the invariant mass of the two leading jets, the energy of the leading jet, and the scalar p_{T} sum of all jets. It is confirmed that all inputs are well modeled in the simulation by performing binned profile-likelihood fits of each input distribution to data. All systematic uncertainties (discussed in section 6) are included in the fit as nuisance parameters. In each case, the goodness of fit is evaluated based on a saturated model [84], as implemented in the CMS

JHEP05(2026)175

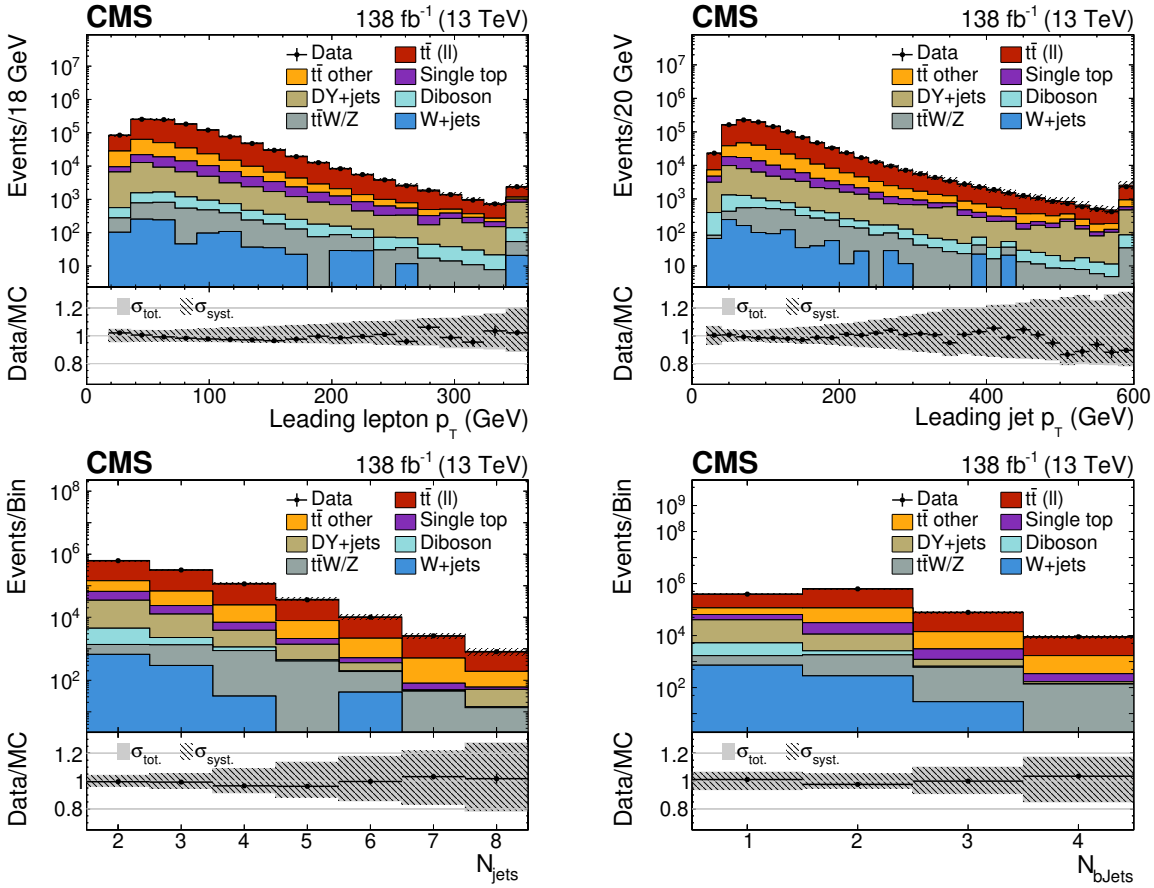

Figure 2. Observed (black markers) and expected (filled histograms) distributions of leading lepton p_{T} (upper left), leading jet p_{T} (upper right), the number of jets (lower left), and the number of b tagged jets (lower right), after event selection. The hatched (grey) areas denote the systematic (total) uncertainties on the expected yields. Vertical and horizontal error bars on the data points represent the statistical uncertainty and the bin width, respectively. Events from all data-taking periods and all channels are combined. The lower panel of each plot shows the ratio between observed and expected distributions. The last bin includes all events above the plotted range.

statistical analysis tool, COMBINE [85]. The procedure is repeated for every 2D distribution of two inputs to ensure a correct description of correlations between inputs by the simulation. Furter details on the goodness-of-fit tests can be found in ref. [86].

The performance of $p_{\mathrm{T,DNN}}^{\mathrm{miss}}$ is compared to $p_{\mathrm{T,PF}}^{\mathrm{miss}}$ and $p_{\mathrm{T,PUPPI}}^{\mathrm{miss}}$ in figure 3, using a simulated sample corresponding to the 2018 data-taking period. The mean (μ) and the resolution (standard deviation, σ) of the difference between $p_{\mathrm{T,gen.}}^{\mathrm{miss}}$ and $p_{\mathrm{T,rec.}}^{\mathrm{miss}}$ is shown as a function of the $p_{\mathrm{T,gen.}}^{\mathrm{miss}}$ and the number of PVs. As a function of both observables, $p_{\mathrm{T,DNN}}^{\mathrm{miss}}$ improves on the resolution, and inclusively it shifts the mean closer to zero in the phase space of this analysis compared to the other $p_{\mathrm{T}}^{\mathrm{miss}}$ reconstruction algorithms. The negative bias at low $p_{\mathrm{T,gen.}}^{\mathrm{miss}}$ arises from the finite $p_{\mathrm{T}}^{\mathrm{miss}}$ resolution which causes the $p_{\mathrm{T,rec.}}^{\mathrm{miss}}$ to be on average larger than $p_{\mathrm{T,gen.}}^{\mathrm{miss}}$ in events with genuinely small $p_{\mathrm{T,gen.}}^{\mathrm{miss}}$ [78]. The DNN can marginally correct for this effect thanks to a better $p_{\mathrm{T}}^{\mathrm{miss}}$ resolution. Overall, the resolution of $p_{\mathrm{T}}^{\mathrm{miss}}$ is improved by approximately 15% by the DNN with respect to $p_{\mathrm{T,PUPPI}}^{\mathrm{miss}}$, while the resolution

JHEP05(2026)175

of $\phi(\vec{p}_{\mathrm{T}}^{\,\mathrm{miss}})$ is improved by around 12%. The improvements allow for a finer binning in the differential measurements of the target observables as they result in a reduction of bin-to-bin migration while ensuring a stable unfolding.

6 Systematic uncertainties

The differential cross section measurements are affected by various sources of systematic uncertainty. They can be grouped into two categories, namely experimental and theoretical uncertainties. The impact of each source is evaluated by varying the uncertainty source by ± 1 standard deviation or by using alternative simulation settings. These variations can affect the response matrix used in the unfolding procedure, as well as the background estimation. For each systematic variation the cross sections are extracted and differences with the nominal values are taken as uncertainties. Because of different detector and/or simulation conditions, dedicated correlation models between different data-taking periods are employed for each source of systematic uncertainty. Unless stated otherwise, the uncertainty is assumed to be fully correlated between different years of data taking.

Experimental uncertainties include those originating from jet reconstruction, corrections applied to simulated samples to improve the shape agreement of data and simulation, normalization of background processes, integrated luminosity measurement, and determination of unclustered energy. The impact from the jet energy scale (JES) uncertainty is estimated by shifting all jet momenta according to seven independent uncertainty sources, which have different treatments of correlations between the data-taking periods. The corresponding shifts in the jet momentum are propagated to $p_{\mathrm{T}}^{\mathrm{miss}}$ [78, 87]. The uncertainty on the jet energy resolution (JER) is introduced when smearing jet energies in simulation to match the resolution observed in data. To evaluate its impact, the smearing is repeated with the JER shifted within its uncertainty. This uncertainty is assumed to be uncorrelated between the data-taking periods.

Correction factors are applied to simulation to account for the differences with data when describing b tagging, lepton selection, lepton energy scale, identification of jets from pileup, trigger selection, and ECAL first level trigger inefficiencies [72]. Each of these correction factors is varied within its uncertainty to estimate its impact on the measured cross section. The statistical component of the uncertainty related to the muon identification efficiency, as well as trigger efficiencies, is considered to be uncorrelated between the data-taking periods. Variations in lepton energy scale are propagated to $p_{\mathrm{T}}^{\mathrm{miss}}$. In addition, the corrections to b tagging efficiencies are re-evaluated separately for systematic variations in JES, JER, identification of jets from pileup, and most of the theoretical uncertainties.

The uncertainties on the integrated luminosities are 1.2, 2.3, and 2.5%, for 2016, 2017, and 2018, respectively, with partial correlations between data-taking periods. This results in a combined uncertainty of 1.6% [39–41].

The distribution of additional pp collisions in simulation is reweighted according to the expected distribution in data assuming a total inelastic pp cross section of 69.2 mb [88]. The reweighting is repeated shifting the inelastic pp cross section by $\pm 4.6\%$ to derive the corresponding uncertainty.

JHEP05(2026)175

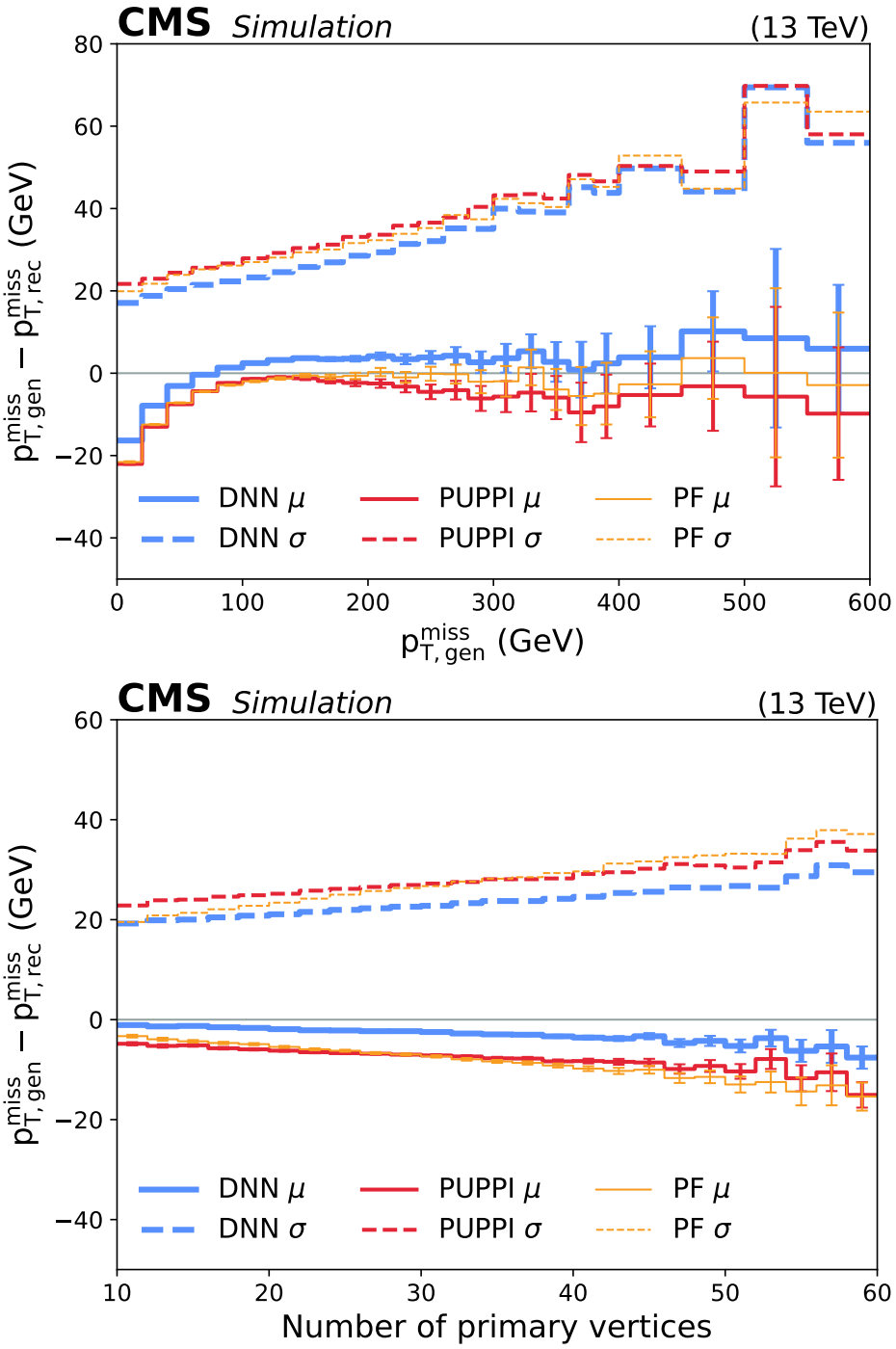

Figure 3. Difference between $p_{\mathrm{T,gen.}}^{\mathrm{miss}}$ and $p_{\mathrm{T,rec.}}^{\mathrm{miss}}$ as a function of the $p_{\mathrm{T,gen.}}^{\mathrm{miss}}$ (upper) and the number of primary vertices (lower) for signal events. The mean difference between the generated and the $p_{\mathrm{T,rec.}}^{\mathrm{miss}}$ per bin is shown as solid line, while the dashed line shows the standard deviation σ, which corresponds to the resolution. The results for $p_{\mathrm{T}}^{\mathrm{miss}}$ corrected by the DNN regression (thick light blue), derived with the PUPPI algorithm (thin red), and the PF algorithm (thinner orange) are shown. A simulated sample for the 2018 data-taking period is used.

JHEP05(2026)175

The normalization of all background processes directly impacts the cross section measurements. The magnitudes of the corresponding uncertainties applied to the normalization are taken from ref. [89]. The largest background contribution, denoted as $\mathrm{t\bar{t}}$ other, is assigned a 5% normalization uncertainty. For single top and DY+jets production, a 20% and a 30% normalization uncertainty is assigned, respectively. Subdominant background processes, such as diboson production, W+jets, and $\mathrm{t\bar{t}W/Z}$ production are assumed to have a 30% normalization uncertainty. Each background normalization is varied individually within the given uncertainty. The simulated samples are normalized to the integrated luminosities of the corresponding data-taking periods [39–41]. The sample normalization is shifted according to the integrated luminosity uncertainties, which are split into uncorrelated and correlated components between the different data-taking periods.

The $p_{\mathrm{T}}^{\mathrm{miss}}$ measurement is affected by energy deposits that remain unclustered. To estimate their impact, the energy from charged and neutral hadrons, as well as photons and hadrons reconstructed in the η region covered by the forward hadron calorimeter, is shifted according to their energy resolutions and propagated to $p_{\mathrm{T}}^{\mathrm{miss}}$. The resulting uncertainty is assumed to be uncorrelated between data-taking periods.

Theoretical uncertainty sources include variations that affect all simulated samples, as well as variations that are only applied to the $\mathrm{t\bar{t}}$ simulation. The impact of initial-state radiation and final-state radiation is estimated by shifting the renormalisation scale for QCD emission in the parton shower by a factor of two and a factor of one half, separately for both initial-state and final-state radiation scales. The uncertainty on the choice of renormalization and factorization scales is estimated in a similar way, shifting the scales up and down by a factor of two, both individually and simultaneously, excluding the configuration where the two scales are shifted simultaneously in opposite directions. The uncertainty on the cross section results is given by the envelope of the corresponding shift variations in the measurements. Uncertainties due to the matching of ME and PS calculations are taken into account by reweighting the nominal $\mathrm{t\bar{t}}$ samples using weights derived with the DNNs using the classification for tuning and reweighting approach [90, 91] to shift the h_{damp} parameter of the POWHEG event generator. This parameter controls the merging between ME and PS and regulates the high p_{T} radiation. The impact of the choice of the scheme to handle the overlap between tW and $\mathrm{t\bar{t}}$ production [56] is estimated by taking the difference between the tW sample based on DR and DS as additional uncertainty into account.

The remaining theoretical uncertainties are only taken into account for the $\mathrm{t\bar{t}}$ simulation. Alternative $\mathrm{t\bar{t}}$ samples are used to estimate the impact of varying the top quark mass by 1 GeV, using different tunes for the underlying event modeling as described in ref. [45], employing two alternative approaches for color reconnection, and enabling early resonance decays [92]. The energy measurement of jets from b quarks is impacted by semileptonic decays of b hadrons. The assumed branching fractions, $\mathcal{B}$, taken from ref. [80], are shifted within the reported uncertainty to estimate the effect on the cross section measurements. The impact of reweighting the top quark p_{T} spectra to NNLO accuracy is evaluated in the cross section measurement by repeating the measurement without the reweighting and taking the difference as a one-sided uncertainty.

JHEP05(2026)175

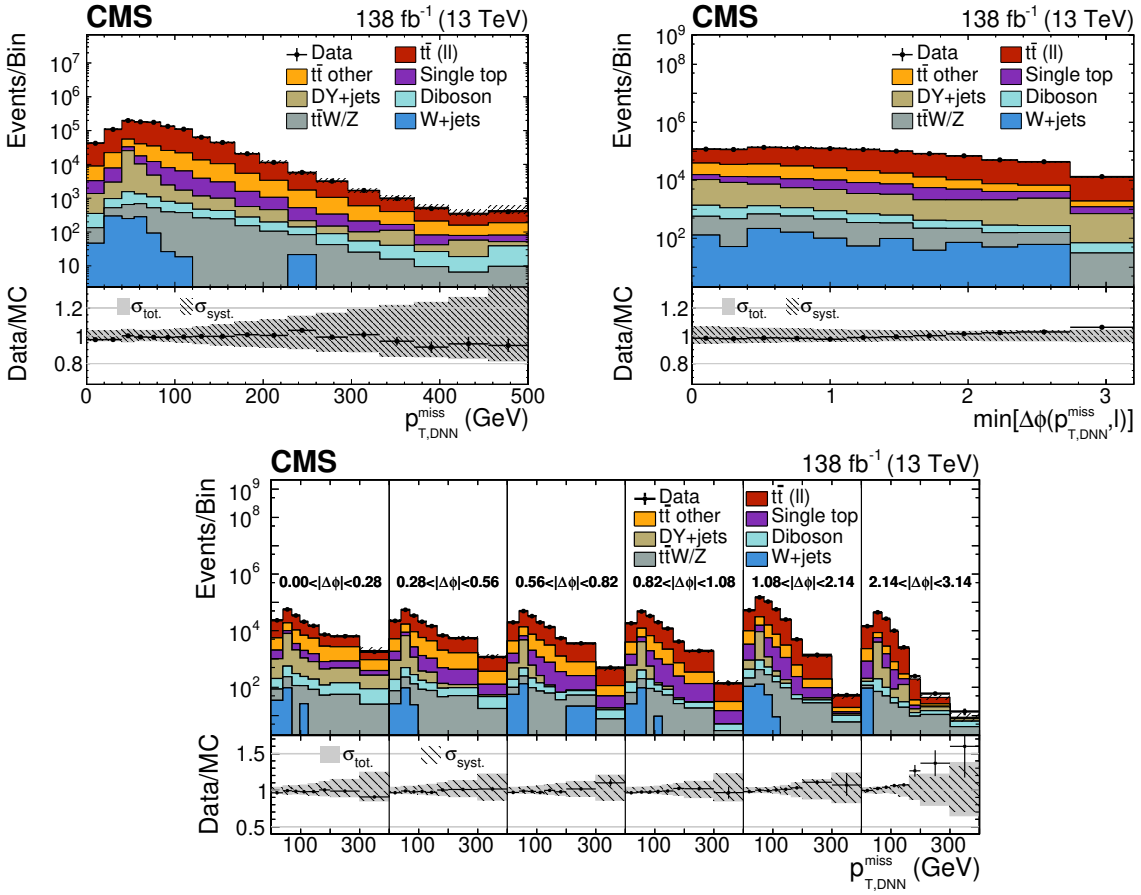

Figure 4. The observed (black markers) and simulated distributions of $p_{\mathrm{T,DNN}}^{\mathrm{miss}}$ (upper left), $\min[\Delta\phi(\vec{p}_{\mathrm{T,DNN}}^{\,\mathrm{miss}}, \vec{p}_{\mathrm{T}}^{\,\ell})]$ (upper right), and the 2D distribution (lower) with both observables are shown. Events from all data-taking periods and all channels are combined. The hatched (grey) areas indicate the systematic (total) uncertainty on the simulation. Vertical and horizontal error bars on the data points represent the statistical uncertainty and the bin width, respectively. The lower panel of each plot shows the ratio of observed data to the expectation from MC simulation in each bin. The last bin includes all events above the plotted range.

Uncertainties associated with the PDF description are evaluated by reweighting the simulated $\mathrm{t\bar{t}}$ sample using weights based on 100 eigenvectors of the NNPDF3.1 Hessian error PDF set [42, 43], keeping the overall normalization fixed. The envelope of all 100 variation shifts is taken as a systematic uncertainty.

7 Results

The detector-level distributions of $p_{\mathrm{T,DNN}}^{\mathrm{miss}}$, $\min[\Delta\phi(\vec{p}_{\mathrm{T,DNN}}^{\,\mathrm{miss}}, \vec{p}_{\mathrm{T}}^{\,\ell})]$, and the 2D distribution of both observables are compared to the expectation from simulation in figure 4. In general, good agreement between the observed data and the simulation is found. For the 2D distribution, a slight over fluctuation at large $\min[\Delta\phi(\vec{p}_{\mathrm{T,DNN}}^{\,\mathrm{miss}}, \vec{p}_{\mathrm{T}}^{\,\ell})]$ and $p_{\mathrm{T,DNN}}^{\mathrm{miss}}$ is found in data, still compatible with simulation considering the large statistical uncertainties in this phase space.

JHEP05(2026)175

Parameter	$e^+e^-/\mu^+\mu^-$	$e^\pm\mu^\mp$
Lepton p_T	>20 GeV	
Lepton $\lvert\eta\rvert$	<2.4	
Number of leptons	=2	
Invariant mass of the two leptons	>20 GeV	
Jet p_T	>30 GeV	
Jet $\lvert\eta\rvert$	<2.4	
ΔR(Jet,Lepton)	>0.4	
Number of b jets	≥2	
Dineutrino transverse momentum ($p_T^{\nu\nu}$)	>40 GeV	—

Table 2. Definition of the fiducial phase space for the same-flavor and the different-flavor channels.

The differential cross sections as functions of $p_T^{\nu\nu}$ and $\min[\Delta\phi(\vec{p}_T^{\,\nu\nu}, \vec{p}_T^{\,\ell})]$ are derived at particle-level by unfolding the detector-level distributions of $p_{T,DNN}^{miss}$ and $\min[\Delta\phi(\vec{p}_{T,DNN}^{\,miss}, \vec{p}_T^{\,\ell})]$ in a fiducial phase space, as described below. The definition of the fiducial phase space summarised in table 2 follows closely the definitions detailed in ref. [89], with the additional requirement of $p_T^{\nu\nu} > 40$ GeV in the same-flavor channels. The momenta of photons within a cone of $\Delta R < 0.1$ around the lepton are added to the lepton momentum, accounting for bremsstrahlung radiations. Particle-level jets containing a B hadron are identified as originating from a b quark. For a better comparison of the measurement with fixed-order predictions, non-prompt neutrinos originating from hadron decays are included in the jet clustering, as recommended in ref. [29]. The binning applied in the final measurements is optimized taking into account the detector resolution, migration effects, and statistical uncertainties. The differential cross section results are extracted from the observed distributions in two steps. In the first step, the estimated contributions from all backgrounds except for $t\bar{t}$ other are subtracted from the observed distributions. In the second step, the observed distributions are unfolded to the fiducial phase space. Within the second step, the contributions from $t\bar{t}$ other are removed by applying a fixed signal fraction per bin, derived based on the ratio of $t\bar{t}$ signal events to all selected $t\bar{t}$ events.

For the unfolding procedure, the TUnfold algorithm [93] is used, performing a least squares minimization without regularization. The choice of the method is motivated by dedicated unfolding studies, where distorted particle-level distributions as well as pseudodata based on the alternative MC@NLO+Pythia $t\bar{t}$ sample were unfolded using the nominal response matrix. The selected method showed the most stable performance in comparison with a simple bin-by-bin (BBB) unfolding where only the diagonal elements of the response matrix are taken into account as well as with respect to a least squares minimization with regularization. In addition, closure tests accounting for potential BSM contributions based on the top squark pair production scenario shown in figure 1 were performed, for a top squark mass of 525 GeV and a neutralino mass of 350 GeV. Within these tests, pseudodata based on the sum of the nominal $t\bar{t}$ signal prediction and the prediction for the top squark pair

JHEP05(2026)175

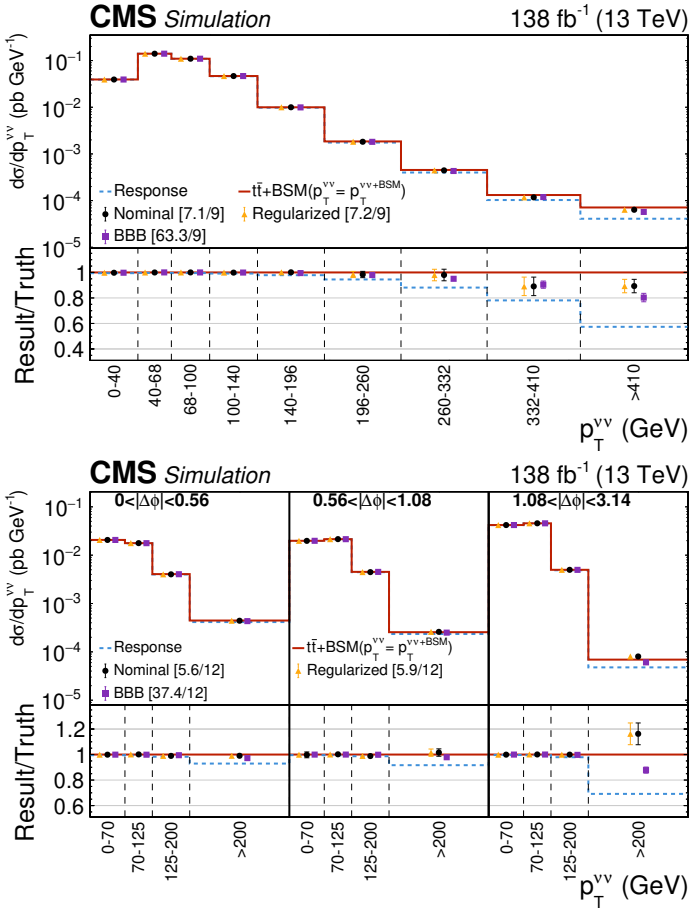

Figure 5. Result of the closure test based on simulation accounting for potential BSM contributions based on a top squark pair production scenario with a stop mass of 525 GeV and a neutralino mass of 350 GeV. The potential BSM contribution is scaled by a factor of ten. The test is performed for the $p_{\mathrm{T}}^{\nu\nu}$ (upper) and 2D measurement (lower) using the nominal (black circles), the regularized (orange triangles), and the bin-by-bin unfolding (purple squares), based on all data-taking periods combined. The unfolded distributions are compared to the expected distribution (red solid line) based on the sum of the nominal dileptonic $\mathrm{t\bar{t}}$ signal sample and BSM signal with the corresponding χ^2/(number of degrees of freedom) values given in the legend in square brackets. The distribution used for the response matrix is shown in blue (dotted line). The error bars correspond to the statistical uncertainty. The lower part shows the ratios between the unfolded and the expected distributions.

production scenario scaled up by an additional factor of ten were unfolded using the nominal response matrix. The corresponding results for the $p_{\mathrm{T}}^{\nu\nu}$ and the 2D distribution can be found in figure 5. Based on the nominal unfolding approach, the expected distributions, where both neutralinos are included in the particle-level definition, can be correctly reproduced. This result confirms that the measurement reproduces deviations from the distribution assumed in the MC simulation, which was used in the construction of the response matrix. The normalized differential cross sections are also derived, with the measured cross section in each bin divided by the total fiducial cross section, allowing for the reduction of several systematic uncertainties.

JHEP05(2026)175

The impact of the systematic uncertainties on the cross section measurements is shown in figure 6. For the $p_{\mathrm{T}}^{\nu\nu}$ measurement, JES is the dominant experimental uncertainty for most of the bins. At large $p_{\mathrm{T}}^{\nu\nu}$, the choice of the tW–$\mathrm{t\bar{t}}$ overlap removal scheme is the largest uncertainty contribution, followed by the normalization of the single top production background and the ME scale, which also mainly affects the single top background estimation. For the $\min[\Delta\phi(\vec{p}_{\mathrm{T}}^{\,\nu\nu}, \vec{p}_{\mathrm{T}}^{\,\ell})]$ measurement, the JES uncertainty is dominant at low values, while at large distances the uncertainty related to the lepton reconstruction has the largest contribution. The 2D measurement shows similar behavior to the $p_{\mathrm{T}}^{\nu\nu}$ measurement, i.e., for most bins the uncertainty associated with JES has the largest contribution. At large $p_{\mathrm{T}}^{\nu\nu}$ in the lowest $\min[\Delta\phi(\vec{p}_{\mathrm{T}}^{\,\nu\nu}, \vec{p}_{\mathrm{T}}^{\,\ell})]$ bin, the choice of the tW–$\mathrm{t\bar{t}}$ overlap removal scheme is the dominant uncertainty. For the bin with the highest $p_{\mathrm{T}}^{\nu\nu}$ and $\min[\Delta\phi(\vec{p}_{\mathrm{T}}^{\,\nu\nu}, \vec{p}_{\mathrm{T}}^{\,\ell})]$, sizeable contributions also arise from the ME-PS matching and ME scale uncertainties.

The bin-to-bin correlations between different sources of uncertainties are extracted from the covariance matrices that include separate terms for statistical and systematic contributions. The statistical component, encoding uncertainties after the unfolding, may contain off-diagonal elements originating from correlations introduced in the unfolding procedure. The same matrices are used to calculate χ^2 values when comparing predictions to the measured results. The procedure of constructing the covariance matrices is described in detail in appendix A of ref. [89].

The measured differential cross sections are compared to five theoretical predictions, namely predictions from the POWHEG+PYTHIA, POWHEG+HERWIG, and MC@NLO+PYTHIA $\mathrm{t\bar{t}}$ samples, and fixed-order calculations [29] at NLO and NNLO accuracy in QCD. The fixed-order calculations use the narrow-width approximation for the top quark decays and include ME scale uncertainties and, in case of the NNLO prediction, also PDF uncertainties. For the three MC-based predictions, a normalization uncertainty of 5% as well as ME scale uncertainties are taken into account. For the NLO MC simulations, only the acceptance and efficiency effects for the fiducial volume are considered. More details on the cross section extraction can be found in ref. [89], which only differs in the choice of regularization.

The differential signal cross sections and their comparisons to the theoretical predictions are shown in figures 7–8. The corresponding χ^2 tests for all measurements, both with and without the inclusion of uncertainties on the predictions, are summarized in table 3, with the corresponding p-values [80] given in table 4.

In general, all predictions are in agreement with the absolute measurements. In the absolute $\min[\Delta\phi(\vec{p}_{\mathrm{T}}^{\,\nu\nu}, \vec{p}_{\mathrm{T}}^{\,\ell})]$ measurement, small shape differences between the measured cross section and the five predictions are observed. These differences match observations from previous measurements of the azimuthal angle between two leptons $\Delta\phi(\ell,\ell)$ [18, 94–98], which is strongly correlated with $\min[\Delta\phi(\vec{p}_{\mathrm{T}}^{\,\nu\nu}, \vec{p}_{\mathrm{T}}^{\,\ell})]$. Slightly larger χ^2/ndf values (where ndf is the number of degrees of freedom) are observed for the 2D differential cross section measurement. While MC@NLO+PYTHIA overpredicts the cross sections in most of the measured bins for the $p_{\mathrm{T}}^{\nu\nu}$ distribution in comparison with other predictions, its χ^2/ndf is found to be close to 1 due to the correlated bin uncertainties. Including the uncertainties on the predictions reduces the χ^2/ndf of most predictions to below unity. Only the MC@NLO+PYTHIA prediction leads to χ^2/ndf values significantly above unity for the normalised 2D measurement. The results

JHEP05(2026)175

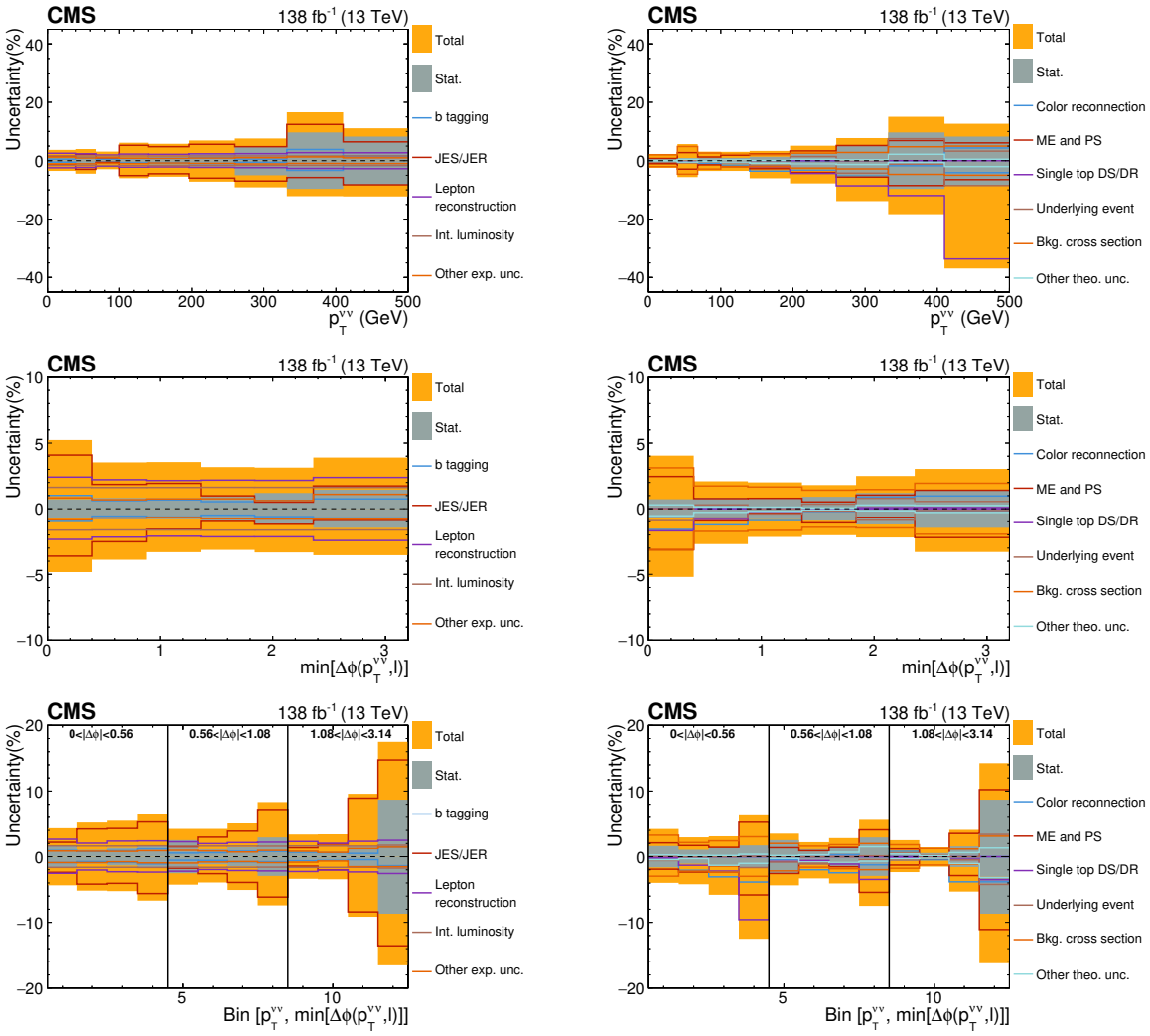

Figure 6. Breakdown of the relative uncertainties from experimental (left) and theoretical (right) sources on the differential cross section measurements as functions of $p_{\mathrm{T}}^{\nu\nu}$ (upper), $\min[\Delta\phi(\vec{p}_{\mathrm{T}}^{\,\nu\nu}, \vec{p}_{\mathrm{T}}^{\,\ell})]$ (middle), and both observables (lower). In the last case, each group of four bins corresponds to $p_{\mathrm{T}}^{\nu\nu}$ bins, and $\min[\Delta\phi(\vec{p}_{\mathrm{T}}^{\,\nu\nu}, \vec{p}_{\mathrm{T}}^{\,\ell})]$ bin edges are indicated by vertical solid lines. The statistical uncertainty (dark grey) takes into account the size of available event counts in both simulated samples and the recorded data. The last bin includes all events above the plotted range.

of the χ^2 tests without including uncertainties show that POWHEG+PYTHIA yields overall the best description for the two one-dimensional absolute differential measurements, and the NNLO calculation shows the best agreement with the 2D absolute result.

For the normalized differential cross sections, shown in figure 8, the systematic uncertainties are slightly smaller than those for the absolute cross section measurements. This especially holds for the $\min[\Delta\phi(\vec{p}_{\mathrm{T}}^{\,\nu\nu}, \vec{p}_{\mathrm{T}}^{\,\ell})]$ measurement, where the dominant uncertainty on the absolute differential measurements that arises from lepton reconstruction efficiency is significantly reduced, which emphasizes the shape differences between the measurement and predictions already discussed for the absolute result. Similar to the absolute results, all predictions are in reasonable agreement with the measurements as shown by the obtained χ^2 values.

JHEP05(2026)175

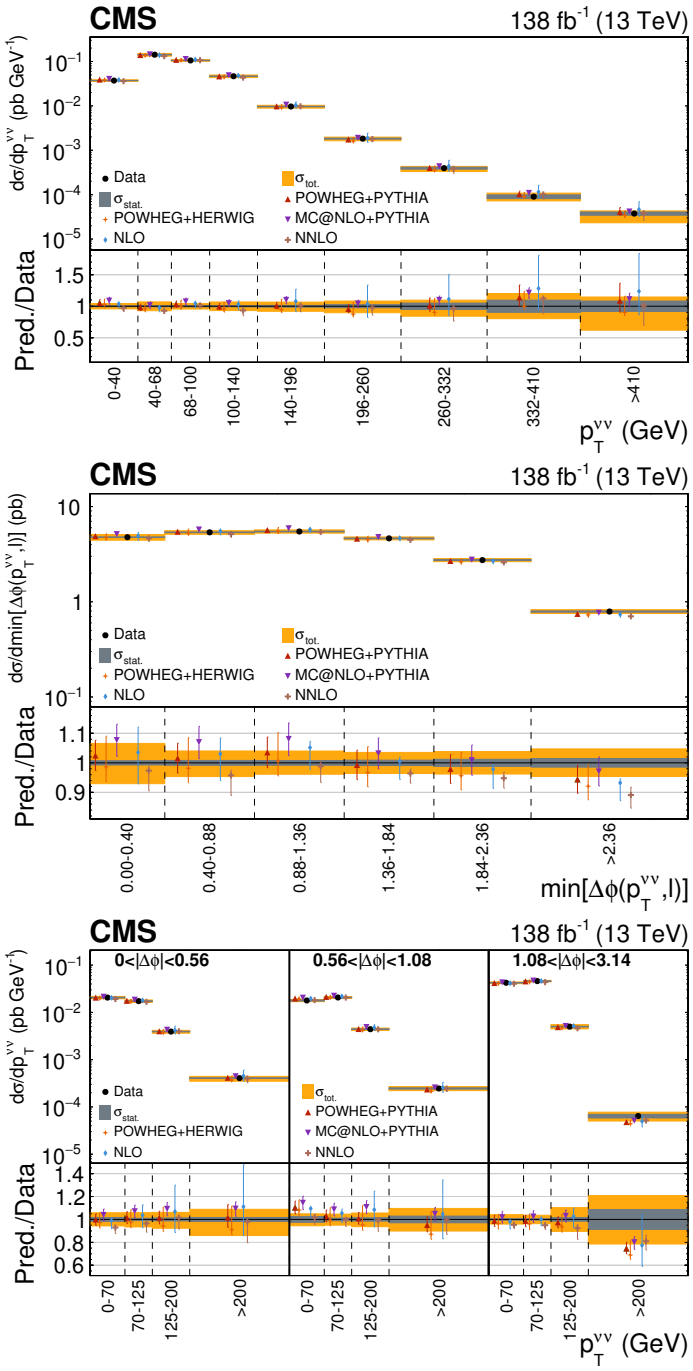

Figure 7. The measured differential signal cross sections (black markers) as functions of $p_{\mathrm{T}}^{\nu\nu}$ (upper), $\min[\Delta\phi(\vec{p}_{\mathrm{T}}^{\,\nu\nu}, \vec{p}_{\mathrm{T}}^{\,\ell})]$ (middle), and double-differential in both observables (lower) are shown. The theoretical predictions from POWHEG+PYTHIA (dark red), POWHEG+HERWIG (orange), MC@NLO+PYTHIA (purple), and the fixed-order NLO (light blue) and NNLO (brown) calculations are compared to the measurement. The cross sections in the last $p_{\mathrm{T}}^{\nu\nu}$ bin of the upper (lower) plot are determined for $p_{\mathrm{T}}^{\nu\nu} > 410$ (200) GeV and normalised to a bin width of 90 (200) GeV for visualisation purposes. The total (statistical) uncertainty on the measurement is shown as an orange (dark grey) band. The lower panel of each plot shows the ratio between theoretical predictions and the measurement.

JHEP05(2026)175

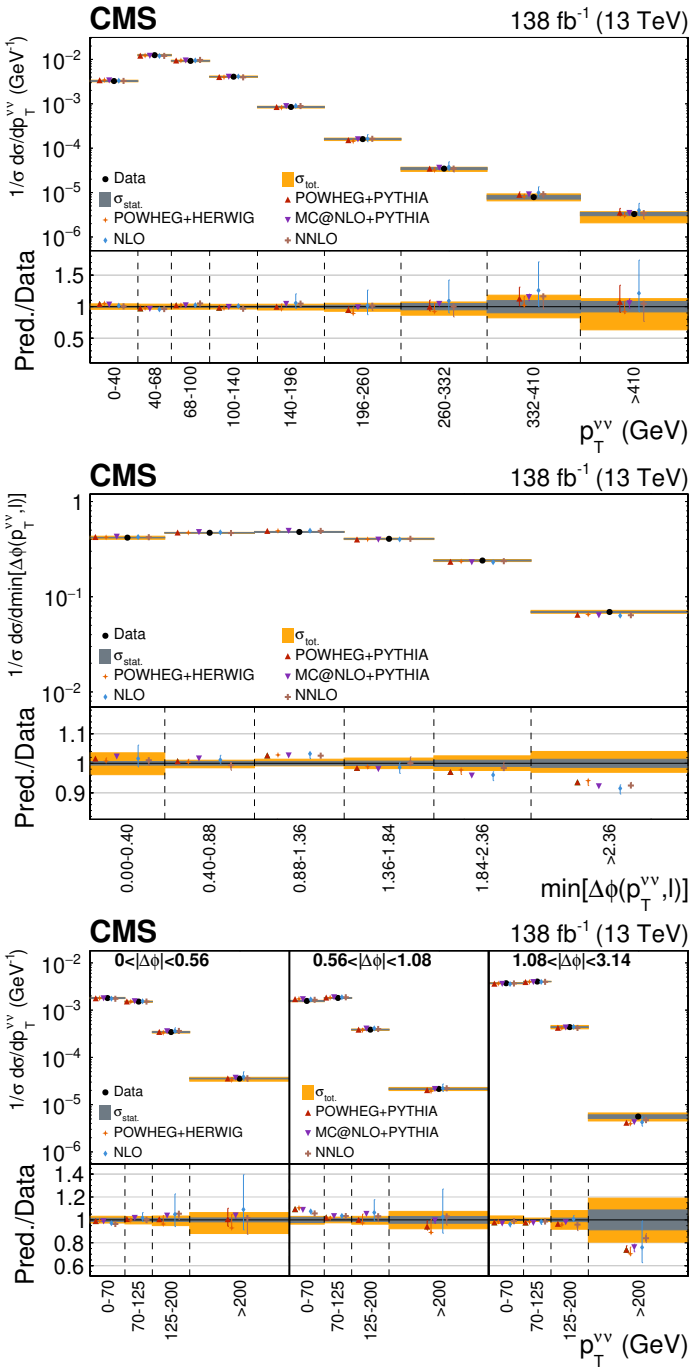

Figure 8. The measured normalized differential signal cross sections (black markers) as functions of $p_{\mathrm{T}}^{\nu\nu}$ (upper), $\min[\Delta\phi(\vec{p}_{\mathrm{T}}^{\,\nu\nu}, \vec{p}_{\mathrm{T}}^{\,\ell})]$ (middle), and double-differential in both observables (lower) are shown. The theoretical predictions from POWHEG+PYTHIA (dark red), POWHEG+HERWIG (orange), MC@NLO+PYTHIA (purple), and the fixed-order NLO (light blue) and NNLO (brown) calculations are compared to the measurement. The cross sections in the last $p_{\mathrm{T}}^{\nu\nu}$ bin of the upper (lower) plot are determined for $p_{\mathrm{T}}^{\nu\nu} > 410$ (200) GeV and normalised to a bin width of 90 (200) GeV for visualisation purposes. The total (statistical) uncertainty on the measurement is shown as an orange (dark grey) band. The lower panel of each plot shows the ratio between theoretical predictions and the measurement.

JHEP05(2026)175

Measurement	ndf	χ^2 (including uncertainties)				
		POWHEG +PYTHIA	POWHEG +HERWIG	MC@NLO +PYTHIA	NLO	NNLO
$p_{\mathrm{T}}^{\nu\nu}$	9	6.8 (1.6)	8.0 (1.0)	9.0 (3.9)	7.1 (1.4)	12.5 (2.5)
$\min[\Delta\phi(\vec{p}_{\mathrm{T}}^{\,\nu\nu}, \vec{p}_{\mathrm{T}}^{\,\ell})]$	6	7.3 (1.5)	7.4 (1.4)	11.5 (2.7)	12.3 (2.5)	11.9 (4.0)
2D	12	18.8 (4.9)	22.4 (3.7)	31.6 (8.6)	24.0 (3.5)	15.8 (4.2)
norm. $p_{\mathrm{T}}^{\nu\nu}$	8	6.4 (3.8)	8.3 (3.2)	6.4 (5.8)	6.7 (1.9)	13.3 (5.5)
norm. $\min[\Delta\phi(\vec{p}_{\mathrm{T}}^{\,\nu\nu}, \vec{p}_{\mathrm{T}}^{\,\ell})]$	5	7.2 (7.0)	7.2 (6.7)	9.2 (8.4)	11.7 (5.4)	11.7 (5.8)
norm. 2D	11	18.1 (16.0)	21.4 (14.5)	28.2 (22.8)	23.1 (7.0)	14.8 (8.5)

Table 3. Results of the χ^2 tests for the absolute and normalized differential cross section measurements for each of the predictions. The χ^2 values including the uncertainties on the predictions are given in parentheses.

Measurement	p-value (including uncertainties)				
	POWHEG +PYTHIA	POWHEG +HERWIG	MC@NLO +PYTHIA	NLO	NNLO
$p_{\mathrm{T}}^{\nu\nu}$	0.66 (1.00)	0.53 (1.00)	0.44 (0.92)	0.63 (1.00)	0.19 (0.98)
$\min[\Delta\phi(\vec{p}_{\mathrm{T}}^{\,\nu\nu}, \vec{p}_{\mathrm{T}}^{\,\ell})]$	0.29 (0.96)	0.28 (0.97)	0.07 (0.84)	0.06 (0.87)	0.07 (0.67)
2D	0.09 (0.96)	0.03 (0.99)	<0.01 (0.73)	0.02 (0.99)	0.20 (0.98)
norm. $p_{\mathrm{T}}^{\nu\nu}$	0.60 (0.87)	0.40 (0.92)	0.60 (0.67)	0.57 (0.98)	0.10 (0.70)
norm. $\min[\Delta\phi(\vec{p}_{\mathrm{T}}^{\,\nu\nu}, \vec{p}_{\mathrm{T}}^{\,\ell})]$	0.21 (0.22)	0.20 (0.24)	0.10 (0.14)	0.04 (0.37)	0.04 (0.33)
norm. 2D	0.08 (0.14)	0.03 (0.21)	<0.01 (0.02)	0.02 (0.80)	0.19 (0.67)

Table 4. The p-value of the χ^2 tests for the absolute and normalized cross section measurements for each of the predictions. The resulting p-values including uncertainties on the predictions are given in parentheses.

8 Summary

Differential cross section measurements have been presented for the top quark pair production in the dileptonic channel in proton-proton (pp) collisions at a center-of-mass energy of 13 TeV using observables based on the dineutrino kinematic properties. The measurements are performed based on the pp collision data recorded by the CMS detector at the CERN LHC between 2016 and 2018, corresponding to an integrated luminosity of 138 fb^{-1}.

The differential cross sections are measured as functions of the transverse momentum of the dineutrino system $p_{\mathrm{T}}^{\nu\nu}$, and the minimal azimuthal angle between the dineutrino system and a charged lepton $\min[\Delta\phi(\vec{p}_{\mathrm{T}}^{\,\nu\nu}, \vec{p}_{\mathrm{T}}^{\,\ell})]$, as well as both observables in two dimensions. To improve the resolution of the missing transverse momentum, which serves as a measure of $p_{\mathrm{T}}^{\nu\nu}$ in signal events, a dedicated deep neural network regression has been developed. The method significantly improves the resolution of both the magnitude and the azimuthal angle

JHEP05(2026)175

of the missing transverse momentum. The absolute and normalized differential cross section results are obtained based on an unregularized least squares unfolding method.

The differential cross sections are compared to predictions based on Monte Carlo simulation as well as two fixed-order theoretical calculations, corresponding to next-to-leading order and next-to-next-to-leading order (NNLO) accuracy in quantum chromodynamics. A remarkable agreement between the different theoretical predictions and the measured differential cross sections is observed. For both one-dimensional measurements, the best overall description is provided by the two POWHEG predictions, while for the two-dimensional measurement the best agreement is observed for the NNLO fixed-order calculation. However, the differences between the five predictions are mostly small, such that none of the predictions is significantly disfavored by the measured differential cross sections. These results constitute the first differential cross section measurements based on the dineutrino kinematic properties in top quark pair production.

Acknowledgments

We congratulate our colleagues in the CERN accelerator departments for the excellent performance of the LHC and thank the technical and administrative staffs at CERN and at other CMS institutes for their contributions to the success of the CMS effort. In addition, we gratefully acknowledge the computing centers and personnel of the Worldwide LHC Computing Grid and other centers for delivering so effectively the computing infrastructure essential to our analyses. Finally, we acknowledge the enduring support for the construction and operation of the LHC, the CMS detector, and the supporting computing infrastructure provided by the following funding agencies: SC (Armenia), BMBWF and FWF (Austria); FNRS and FWO (Belgium); CNPq, CAPES, FAPERJ, FAPERGS, and FAPESP (Brazil); MES and BNSF (Bulgaria); CERN; CAS, MoST, and NSFC (China); MINCIENCIAS (Colombia); MSES and CSF (Croatia); RIF (Cyprus); SENESCYT (Ecuador); ERC PRG, TARISTU24-TK10 and MoER TK202 (Estonia); Academy of Finland, MEC, and HIP (Finland); CEA and CNRS/IN2P3 (France); SRNSF (Georgia); BMFTR, DFG, and HGF (Germany); GSRI (Greece); NKFIH (Hungary); DAE and DST (India); IPM (Iran); SFI (Ireland); INFN (Italy); MSIT and NRF (Republic of Korea); MES (Latvia); LMTLT (Lithuania); MOE and UM (Malaysia); BUAP, CINVESTAV, CONACYT, LNS, SEP, and UASLP-FAI (Mexico); MOS (Montenegro); MBIE (New Zealand); PAEC (Pakistan); MES, NSC, and NAWA (Poland); FCT (Portugal); MESTD (Serbia); MICIU/AEI and PCTI (Spain); MOSTR (Sri Lanka); Swiss Funding Agencies (Switzerland); MST (Taipei); MHESI (Thailand); TUBITAK and TENMAK (Türkiye); NASU (Ukraine); STFC (United Kingdom); DOE and NSF (U.S.A.).

Individuals have received support from the Marie-Curie program and the European Research Council and Horizon 2020 Grant, contract Nos. 675440, 724704, 752730, 758316, 765710, 824093, 101115353, 101002207, 101001205, and COST Action CA16108 (European Union); the Leventis Foundation; the Alfred P. Sloan Foundation; the Alexander von Humboldt Foundation; the Science Committee, project no. 22rl-037 (Armenia); the Fonds pour la Formation à la Recherche dans l'Industrie et dans l'Agriculture (FRIA) and Fonds voor Wetenschappelijk Onderzoek contract No. 1228724N (Belgium); the Beijing Municipal Science & Technology Commission, No. Z191100007219010, the Fundamental Research Funds for the Central Uni-

JHEP05(2026)175

versities, the Ministry of Science and Technology of China under Grant No. 2023YFA1605804, and the Natural Science Foundation of China under Grant No. 12061141002 (China); the Ministry of Education, Youth and Sports (MEYS) of the Czech Republic; the Shota Rustaveli National Science Foundation, grant FR-22-985 (Georgia); the Deutsche Forschungsgemeinschaft (DFG), among others, under Germany's Excellence Strategy – EXC 2121 "Quantum Universe" – 390833306, and under project number 400140256 – GRK2497; the Hellenic Foundation for Research and Innovation (HFRI), Project Number 2288 (Greece); the Hungarian Academy of Sciences, the New National Excellence Program – ÚNKP, the NKFIH research grants K 131991, K 133046, K 138136, K 143460, K 143477, K 146913, K 146914, K 147048, 2020-2.2.1-ED-2021-00181, TKP2021-NKTA-64, and 2021-4.1.2-NEMZ_KI-2024-00036 (Hungary); the Council of Science and Industrial Research, India; ICSC – National Research Center for High Performance Computing, Big Data and Quantum Computing, FAIR – Future Artificial Intelligence Research, and CUP I53D23001070006 (Mission 4 Component 1), funded by the NextGenerationEU program (Italy); the Latvian Council of Science; the Ministry of Education and Science, project no. 2022/WK/14, and the National Science Center, contracts Opus 2021/41/B/ST2/01369, 2021/43/B/ST2/01552, 2023/49/B/ST2/03273, and the NAWA contract BPN/PPO/2021/1/00011 (Poland); the Fundação para a Ciência e a Tecnologia, grant CEECIND/01334/2018 (Portugal); the National Priorities Research Program by Qatar National Research Fund; MICIU/AEI/10.13039/501100011033, ERDF/EU, "European Union NextGenerationEU/PRTR", and Programa Severo Ochoa del Principado de Asturias (Spain); the Chulalongkorn Academic into Its 2nd Century Project Advancement Project, the National Science, Research and Innovation Fund program IND_FF_68_369_2300_097, and the Program Management Unit for Human Resources & Institutional Development, Research and Innovation, grant B39G680009 (Thailand); the Kavli Foundation; the Nvidia Corporation; the SuperMicro Corporation; the Welch Foundation, contract C-1845; and the Weston Havens Foundation (U.S.A.).

Data Availability Statement. Release and preservation of data used by the CMS Collaboration as the basis for publications is guided by the CMS data preservation, re-use and open access policy.

Code Availability Statement. The CMS core software is publicly available on GitHub.

References

[1] ATLAS collaboration, *Measurements of top quark pair relative differential cross-sections with ATLAS in pp collisions at* $\sqrt{s} = 7$ *TeV*, *Eur. Phys. J. C* **73** (2013) 2261 [arXiv:1207.5644] [INSPIRE].

[2] CMS collaboration, *Measurement of Differential Top-Quark Pair Production Cross Sections in pp collisions at* $\sqrt{s} = 7$ *TeV*, *Eur. Phys. J. C* **73** (2013) 2339 [arXiv:1211.2220] [INSPIRE].

JHEP05(2026)175

[3] ATLAS collaboration, *Measurements of normalized differential cross sections for $t\bar{t}$ production in pp collisions at $\sqrt{s} = 7$ TeV using the ATLAS detector*, *Phys. Rev. D* **90** (2014) 072004 [arXiv:1407.0371] [INSPIRE].

[4] ATLAS collaboration, *Differential top-antitop cross-section measurements as a function of observables constructed from final-state particles using pp collisions at $\sqrt{s} = 7$ TeV in the ATLAS detector*, *JHEP* **06** (2015) 100 [arXiv:1502.05923] [INSPIRE].

[5] ATLAS collaboration, *Measurement of top quark pair differential cross-sections in the dilepton channel in pp collisions at $\sqrt{s} = 7$ and 8 TeV with ATLAS*, *Phys. Rev. D* **94** (2016) 092003 [*Addendum ibid.* **101** (2020) 119901] [arXiv:1607.07281] [INSPIRE].

[6] CMS collaboration, *Measurement of the differential cross section for top quark pair production in pp collisions at $\sqrt{s} = 8$ TeV*, *Eur. Phys. J. C* **75** (2015) 542 [arXiv:1505.04480] [INSPIRE].

[7] ATLAS collaboration, *Measurements of top-quark pair differential cross-sections in the lepton+jets channel in pp collisions at $\sqrt{s} = 8$ TeV using the ATLAS detector*, *Eur. Phys. J. C* **76** (2016) 538 [arXiv:1511.04716] [INSPIRE].

[8] ATLAS collaboration, *Measurement of the differential cross-section of highly boosted top quarks as a function of their transverse momentum in $\sqrt{s} = 8$ TeV proton-proton collisions using the ATLAS detector*, *Phys. Rev. D* **93** (2016) 032009 [arXiv:1510.03818] [INSPIRE].

[9] CMS collaboration, *Measurement of the $t\bar{t}$ production cross section in the all-jets final state in pp collisions at $\sqrt{s} = 8$ TeV*, *Eur. Phys. J. C* **76** (2016) 128 [arXiv:1509.06076] [INSPIRE].

[10] CMS collaboration, *Measurement of the integrated and differential $t\bar{t}$ production cross sections for high-p_t top quarks in pp collisions at $\sqrt{s} = 8$ TeV*, *Phys. Rev. D* **94** (2016) 072002 [arXiv:1605.00116] [INSPIRE].

[11] CMS collaboration, *Measurement of double-differential cross sections for top quark pair production in pp collisions at $\sqrt{s} = 8$ TeV and impact on parton distribution functions*, *Eur. Phys. J. C* **77** (2017) 459 [arXiv:1703.01630] [INSPIRE].

[12] ATLAS collaboration, *Measurement of the top-quark mass in $t\bar{t} + 1$-jet events collected with the ATLAS detector in pp collisions at $\sqrt{s} = 8$ TeV*, *JHEP* **11** (2019) 150 [arXiv:1905.02302] [INSPIRE].

[13] CMS collaboration, *Measurement of differential cross sections for top quark pair production using the lepton+jets final state in proton-proton collisions at 13 TeV*, *Phys. Rev. D* **95** (2017) 092001 [arXiv:1610.04191] [INSPIRE].

[14] ATLAS collaboration, *Measurement of jet activity produced in top-quark events with an electron, a muon and two b-tagged jets in the final state in pp collisions at $\sqrt{s} = 13$ TeV with the ATLAS detector*, *Eur. Phys. J. C* **77** (2017) 220 [arXiv:1610.09978] [INSPIRE].

[15] ATLAS collaboration, *Measurements of top-quark pair differential cross-sections in the $e\mu$ channel in pp collisions at $\sqrt{s} = 13$ TeV using the ATLAS detector*, *Eur. Phys. J. C* **77** (2017) 292 [arXiv:1612.05220] [INSPIRE].

[16] CMS collaboration, *Measurement of normalized differential $t\bar{t}$ cross sections in the dilepton channel from pp collisions at $\sqrt{s} = 13$ TeV*, *JHEP* **04** (2018) 060 [arXiv:1708.07638] [INSPIRE].

[17] CMS collaboration, *Measurement of differential cross sections for the production of top quark pairs and of additional jets in lepton+jets events from pp collisions at $\sqrt{s} = 13$ TeV*, *Phys. Rev. D* **97** (2018) 112003 [arXiv:1803.08856] [INSPIRE].

JHEP05(2026)175

[18] CMS collaboration, *Measurements of $t\bar{t}$ differential cross sections in proton-proton collisions at $\sqrt{s} = 13$ TeV using events containing two leptons*, *JHEP* **02** (2019) 149 [arXiv:1811.06625] [INSPIRE].

[19] CMS collaboration, *Measurement of $t\bar{t}$ normalised multi-differential cross sections in pp collisions at $\sqrt{s} = 13$ TeV, and simultaneous determination of the strong coupling strength, top quark pole mass, and parton distribution functions*, *Eur. Phys. J. C* **80** (2020) 658 [arXiv:1904.05237] [INSPIRE].

[20] ATLAS collaboration, *Measurements of top-quark pair differential and double-differential cross-sections in the ℓ+jets channel with pp collisions at $\sqrt{s} = 13$ TeV using the ATLAS detector*, *Eur. Phys. J. C* **79** (2019) 1028 [*Erratum ibid.* **80** (2020) 1092] [arXiv:1908.07305] [INSPIRE].

[21] ATLAS collaboration, *Measurement of the $t\bar{t}$ production cross-section and lepton differential distributions in $e\mu$ dilepton events from pp collisions at $\sqrt{s} = 13$ TeV with the ATLAS detector*, *Eur. Phys. J. C* **80** (2020) 528 [arXiv:1910.08819] [INSPIRE].

[22] ATLAS collaboration, *Measurements of top-quark pair single- and double-differential cross-sections in the all-hadronic channel in pp collisions at $\sqrt{s} = 13$ TeV using the ATLAS detector*, *JHEP* **01** (2021) 033 [arXiv:2006.09274] [INSPIRE].

[23] CMS collaboration, *Measurement of differential $t\bar{t}$ production cross sections in the full kinematic range using lepton+jets events from proton-proton collisions at $\sqrt{s} = 13$ TeV*, *Phys. Rev. D* **104** (2021) 092013 [arXiv:2108.02803] [INSPIRE].

[24] S. Weinberg, *Supersymmetry at Ordinary Energies. 1. Masses and Conservation Laws*, *Phys. Rev. D* **26** (1982) 287 [INSPIRE].

[25] W. Beenakker et al., *NNLL resummation for stop pair-production at the LHC*, *JHEP* **05** (2016) 153 [arXiv:1601.02954] [INSPIRE].

[26] CMS collaboration, *Search for top squark pair production using dilepton final states in pp collision data collected at $\sqrt{s} = 13$ TeV*, *Eur. Phys. J. C* **81** (2021) 3 [arXiv:2008.05936] [INSPIRE].

[27] CMS collaboration, *Combined searches for the production of supersymmetric top quark partners in proton-proton collisions at $\sqrt{s} = 13$ TeV*, *Eur. Phys. J. C* **81** (2021) 970 [arXiv:2107.10892] [INSPIRE].

[28] ATLAS collaboration, *Search for direct top squark pair production in final states with two leptons in $\sqrt{s} = 13$ TeV pp collisions with the ATLAS detector*, *Eur. Phys. J. C* **77** (2017) 898 [arXiv:1708.03247] [INSPIRE].

[29] M. Czakon, A. Mitov and R. Poncelet, *NNLO QCD corrections to leptonic observables in top-quark pair production and decay*, *JHEP* **05** (2021) 212 [arXiv:2008.11133] [INSPIRE].

[30] HEPData record for this analysis, (2025), DOI:10.17182/hepdata.153302.

[31] CMS collaboration, *The CMS Experiment at the CERN LHC*, 2008 *JINST* **3** S08004 [INSPIRE].

[32] CMS collaboration, *Development of the CMS detector for the CERN LHC Run 3*, 2024 *JINST* **19** P05064 [arXiv:2309.05466] [INSPIRE].

[33] CMS collaboration, *Performance of the CMS Level-1 trigger in proton-proton collisions at $\sqrt{s} = 13$ TeV*, 2020 *JINST* **15** P10017 [arXiv:2006.10165] [INSPIRE].

[34] CMS collaboration, *The CMS trigger system*, 2017 *JINST* **12** P01020 [arXiv:1609.02366] [INSPIRE].

JHEP05(2026)175

[35] CMS collaboration, *Performance of the CMS high-level trigger during LHC Run 2*, 2024 *JINST* **19** P11021 [arXiv:2410.17038] [INSPIRE].

[36] CMS collaboration, *Electron and photon reconstruction and identification with the CMS experiment at the CERN LHC*, 2021 *JINST* **16** P05014 [arXiv:2012.06888] [INSPIRE].

[37] CMS collaboration, *Performance of the CMS muon detector and muon reconstruction with proton-proton collisions at* $\sqrt{s} = 13$ *TeV*, 2018 *JINST* **13** P06015 [arXiv:1804.04528] [INSPIRE].

[38] CMS collaboration, *Description and Performance of Track and Primary-Vertex Reconstruction with the CMS Tracker*, 2014 *JINST* **9** P10009 [arXiv:1405.6569] [INSPIRE].

[39] CMS collaboration, *Precision luminosity measurement in proton-proton collisions at* $\sqrt{s} = 13$ *TeV in 2015 and 2016 at CMS*, *Eur. Phys. J. C* **81** (2021) 800 [arXiv:2104.01927] [INSPIRE].

[40] CMS collaboration, *CMS luminosity measurement for the 2017 data-taking period at* $\sqrt{s} = 13$ *TeV*, CMS-PAS-LUM-17-004 (2018) [INSPIRE].

[41] CMS collaboration, *CMS luminosity measurement for the 2018 data-taking period at* $\sqrt{s} = 13$ *TeV*, CMS-PAS-LUM-18-002 (2019) [INSPIRE].

[42] NNPDF collaboration, *Unbiased global determination of parton distributions and their uncertainties at NNLO and at LO*, *Nucl. Phys. B* **855** (2012) 153 [arXiv:1107.2652] [INSPIRE].

[43] NNPDF collaboration, *Parton distributions from high-precision collider data*, *Eur. Phys. J. C* **77** (2017) 663 [arXiv:1706.00428] [INSPIRE].

[44] T. Sjöstrand et al., *An introduction to PYTHIA 8.2*, *Comput. Phys. Commun.* **191** (2015) 159 [arXiv:1410.3012] [INSPIRE].

[45] CMS collaboration, *Extraction and validation of a new set of CMS PYTHIA8 tunes from underlying-event measurements*, *Eur. Phys. J. C* **80** (2020) 4 [arXiv:1903.12179] [INSPIRE].

[46] GEANT4 collaboration, *GEANT4 — A Simulation Toolkit*, *Nucl. Instrum. Meth. A* **506** (2003) 250 [INSPIRE].

[47] P. Nason, *A new method for combining NLO QCD with shower Monte Carlo algorithms*, *JHEP* **11** (2004) 040 [hep-ph/0409146] [INSPIRE].

[48] S. Frixione, P. Nason and C. Oleari, *Matching NLO QCD computations with Parton Shower simulations: the POWHEG method*, *JHEP* **11** (2007) 070 [arXiv:0709.2092] [INSPIRE].

[49] S. Alioli, P. Nason, C. Oleari and E. Re, *A general framework for implementing NLO calculations in shower Monte Carlo programs: the POWHEG BOX*, *JHEP* **06** (2010) 043 [arXiv:1002.2581] [INSPIRE].

[50] J. Alwall et al., *The automated computation of tree-level and next-to-leading order differential cross sections, and their matching to parton shower simulations*, *JHEP* **07** (2014) 079 [arXiv:1405.0301] [INSPIRE].

[51] R. Frederix and S. Frixione, *Merging meets matching in MC@NLO*, *JHEP* **12** (2012) 061 [arXiv:1209.6215] [INSPIRE].

[52] J. Bellm et al., *Herwig 7.0/Herwig++ 3.0 release note*, *Eur. Phys. J. C* **76** (2016) 196 [arXiv:1512.01178] [INSPIRE].

[53] CMS collaboration, *Development and validation of HERWIG 7 tunes from CMS underlying-event measurements*, *Eur. Phys. J. C* **81** (2021) 312 [arXiv:2011.03422] [INSPIRE].

JHEP05(2026)175

[54] J. Alwall et al., *Comparative study of various algorithms for the merging of parton showers and matrix elements in hadronic collisions*, *Eur. Phys. J. C* **53** (2008) 473 [arXiv:0706.2569] [INSPIRE].

[55] S. Alioli, P. Nason, C. Oleari and E. Re, *NLO single-top production matched with shower in POWHEG: s- and t-channel contributions*, *JHEP* **09** (2009) 111 [*Erratum ibid.* **02** (2010) 011] [arXiv:0907.4076] [INSPIRE].

[56] E. Re, *Single-top Wt-channel production matched with parton showers using the POWHEG method*, *Eur. Phys. J. C* **71** (2011) 1547 [arXiv:1009.2450] [INSPIRE].

[57] M. Czakon and A. Mitov, *Top++: A Program for the Calculation of the Top-Pair Cross-Section at Hadron Colliders*, *Comput. Phys. Commun.* **185** (2014) 2930 [arXiv:1112.5675] [INSPIRE].

[58] M. Czakon, P. Fiedler and A. Mitov, *Total Top-Quark Pair-Production Cross Section at Hadron Colliders Through* $O(\alpha_S^4)$, *Phys. Rev. Lett.* **110** (2013) 252004 [arXiv:1303.6254] [INSPIRE].

[59] M. Cacciari et al., *Top-pair production at hadron colliders with next-to-next-to-leading logarithmic soft-gluon resummation*, *Phys. Lett. B* **710** (2012) 612 [arXiv:1111.5869] [INSPIRE].

[60] P. Bärnreuther, M. Czakon and A. Mitov, *Percent Level Precision Physics at the Tevatron: First Genuine NNLO QCD Corrections to* $q\bar{q} \to t\bar{t} + X$, *Phys. Rev. Lett.* **109** (2012) 132001 [arXiv:1204.5201] [INSPIRE].

[61] M. Czakon and A. Mitov, *NNLO corrections to top-pair production at hadron colliders: the all-fermionic scattering channels*, *JHEP* **12** (2012) 054 [arXiv:1207.0236] [INSPIRE].

[62] M. Czakon et al., *Top-pair production at the LHC through NNLO QCD and NLO EW*, *JHEP* **10** (2017) 186 [arXiv:1705.04105] [INSPIRE].

[63] R. Gavin, Y. Li, F. Petriello and S. Quackenbush, *FEWZ 2.0: A code for hadronic Z production at next-to-next-to-leading order*, *Comput. Phys. Commun.* **182** (2011) 2388 [arXiv:1011.3540] [INSPIRE].

[64] Y. Li and F. Petriello, *Combining QCD and electroweak corrections to dilepton production in FEWZ*, *Phys. Rev. D* **86** (2012) 094034 [arXiv:1208.5967] [INSPIRE].

[65] N. Kidonakis, *Two-loop soft anomalous dimensions for single top quark associated production with a* W^- *or* H^-, *Phys. Rev. D* **82** (2010) 054018 [arXiv:1005.4451] [INSPIRE].

[66] M. Aliev et al., *HATHOR: HAdronic Top and Heavy quarks crOss section calculatoR*, *Comput. Phys. Commun.* **182** (2011) 1034 [arXiv:1007.1327] [INSPIRE].

[67] P. Kant et al., *HatHor for single top-quark production: Updated predictions and uncertainty estimates for single top-quark production in hadronic collisions*, *Comput. Phys. Commun.* **191** (2015) 74 [arXiv:1406.4403] [INSPIRE].

[68] T. Gehrmann et al., W^+W^- *Production at Hadron Colliders in Next to Next to Leading Order QCD*, *Phys. Rev. Lett.* **113** (2014) 212001 [arXiv:1408.5243] [INSPIRE].

[69] J.M. Campbell, R.K. Ellis and C. Williams, *Vector Boson Pair Production at the LHC*, *JHEP* **07** (2011) 018 [arXiv:1105.0020] [INSPIRE].

[70] D. Contardo et al., *Technical Proposal for the Phase-II Upgrade of the CMS Detector*, CERN-LHCC-2015-010 (2015) [DOI:10.17181/CERN.VU8I.D59J] [INSPIRE].

[71] CMS collaboration, *Particle-flow reconstruction and global event description with the CMS detector*, 2017 *JINST* **12** P10003 [arXiv:1706.04965] [INSPIRE].

[72] CMS collaboration, *Performance of the CMS electromagnetic calorimeter in pp collisions at* $\sqrt{s} = 13$ *TeV*, 2024 *JINST* **19** P09004 [arXiv:2403.15518] [INSPIRE].

JHEP05(2026)175

[73] CMS collaboration, *Performance of CMS muon reconstruction from proton-proton to heavy ion collisions*, 2024 *JINST* **19** P09012 [arXiv:2404.17377] [INSPIRE].

[74] M. Cacciari, G.P. Salam and G. Soyez, *The anti-k_t jet clustering algorithm*, *JHEP* **04** (2008) 063 [arXiv:0802.1189] [INSPIRE].

[75] M. Cacciari, G.P. Salam and G. Soyez, *FastJet User Manual*, *Eur. Phys. J. C* **72** (2012) 1896 [arXiv:1111.6097] [INSPIRE].

[76] CMS collaboration, *Pileup mitigation at CMS in 13 TeV data*, 2020 *JINST* **15** P09018 [arXiv:2003.00503] [INSPIRE].

[77] E. Bols et al., *Jet Flavour Classification Using DeepJet*, 2020 *JINST* **15** P12012 [arXiv:2008.10519] [INSPIRE].

[78] CMS collaboration, *Performance of missing transverse momentum reconstruction in proton-proton collisions at $\sqrt{s} = 13$ TeV using the CMS detector*, 2019 *JINST* **14** P07004 [arXiv:1903.06078] [INSPIRE].

[79] D. Bertolini, P. Harris, M. Low and N. Tran, *Pileup Per Particle Identification*, *JHEP* **10** (2014) 059 [arXiv:1407.6013] [INSPIRE].

[80] Particle Data Group collaboration, *Review of particle physics*, *Phys. Rev. D* **110** (2024) 030001 [INSPIRE].

[81] CMS collaboration, *Identification of heavy-flavour jets with the CMS detector in pp collisions at 13 TeV*, 2018 *JINST* **13** P05011 [arXiv:1712.07158] [INSPIRE].

[82] M. Abadi et al., *TensorFlow: Large-Scale Machine Learning on Heterogeneous Distributed Systems*, arXiv:1603.04467 [DOI:10.5281/zenodo.4724125] [INSPIRE].

[83] F. Chollet et al., *keras*, https://keras.io, (2015).

[84] R. Cousins, *Generalization of chisquare goodness-of-fit test for binned data using saturated models, with application to histograms*, https://www.physics.ucla.edu/~cousins/stats/cousins_saturated.pdf (2013).

[85] CMS collaboration, *The CMS Statistical Analysis and Combination Tool: Combine*, *Comput. Softw. Big Sci.* **8** (2024) 19 [arXiv:2404.06614] [INSPIRE].

[86] D. Meuser, *Measurement of the differential dileptonic $t\bar{t}$ cross section in a BSM phase space with the CMS detector using the full LHC Run 2 data set*, Ph.D. thesis, RWTH Aachen University, RWTH Aachen University, Aachen, Tech. Hochsch., Germany (2023) [DOI:10.18154/RWTH-2023-11969] [INSPIRE].

[87] CMS collaboration, *Jet energy scale and resolution in the CMS experiment in pp collisions at 8 TeV*, 2017 *JINST* **12** P02014 [arXiv:1607.03663] [INSPIRE].

[88] CMS collaboration, *Measurement of the inelastic proton-proton cross section at $\sqrt{s} = 13$ TeV*, *JHEP* **07** (2018) 161 [arXiv:1802.02613] [INSPIRE].

[89] CMS collaboration, *Differential cross section measurements for the production of top quark pairs and of additional jets using dilepton events from pp collisions at $\sqrt{s} = 13$ TeV*, *JHEP* **02** (2025) 064 [arXiv:2402.08486] [INSPIRE].

[90] A. Andreassen and B. Nachman, *Neural Networks for Full Phase-space Reweighting and Parameter Tuning*, *Phys. Rev. D* **101** (2020) 091901 [arXiv:1907.08209] [INSPIRE].

[91] CMS collaboration, *Reweighting simulated events using machine-learning techniques in the CMS experiment*, *Eur. Phys. J. C* **85** (2025) 495 [arXiv:2411.03023] [INSPIRE].

JHEP05(2026)175

[92] CMS collaboration, *CMS pythia 8 colour reconnection tunes based on underlying-event data*, *Eur. Phys. J. C* **83** (2023) 587 [arXiv:2205.02905] [INSPIRE].

[93] S. Schmitt, *TUnfold: an algorithm for correcting migration effects in high energy physics*, 2012 *JINST* **7** T10003 [arXiv:1205.6201] [INSPIRE].

[94] ATLAS collaboration, *Inclusive and differential cross-sections for dilepton $t\bar{t}$ production measured in $\sqrt{s} = 13$ TeV pp collisions with the ATLAS detector*, *JHEP* **07** (2023) 141 [arXiv:2303.15340] [INSPIRE].

[95] ATLAS collaboration, *Measurements of top quark spin observables in $t\bar{t}$ events using dilepton final states in $\sqrt{s} = 8$ TeV pp collisions with the ATLAS detector*, *JHEP* **03** (2017) 113 [arXiv:1612.07004] [INSPIRE].

[96] ATLAS collaboration, *Measurements of top-quark pair spin correlations in the $e\mu$ channel at $\sqrt{s} = 13$ TeV using pp collisions in the ATLAS detector*, *Eur. Phys. J. C* **80** (2020) 754 [arXiv:1903.07570] [INSPIRE].

[97] CMS collaboration, *Measurements of $t\bar{t}$ spin correlations and top quark polarization using dilepton final states in pp collisions at $\sqrt{s} = 8$ TeV*, *Phys. Rev. D* **93** (2016) 052007 [arXiv:1601.01107] [INSPIRE].

[98] CMS collaboration, *Measurement of the top quark polarization and $t\bar{t}$ spin correlations using dilepton final states in proton-proton collisions at $\sqrt{s} = 13$ TeV*, *Phys. Rev. D* **100** (2019) 072002 [arXiv:1907.03729] [INSPIRE].

JHEP05(2026)175

The CMS collaboration

V. Chekhovsky[1], A. Hayrapetyan[1], V. Makarenko[1], A. Tumasyan[1,a], W. Adam[2], J.W. Andrejkovic[2], L. Benato[2], T. Bergauer[2], K. Damanakis[2], M. Dragicevic[2], P.S. Hussain[2], M. Jeitler[2,b], N. Krammer[2], A. Li[2], D. Liko[2], I. Mikulec[2], J. Schieck[2,b], D. Schwarz[2], R. Schöfbeck[2,b], M. Sonawane[2], W. Waltenberger[2], C.-E. Wulz[2,b], T. Janssen[3], H. Kwon[3], T. Van Laer[3], P. Van Mechelen[3], N. Breugelmans[4], J. D'Hondt[4], S. Dansana[4], A. De Moor[4], M. Delcourt[4], F. Heyen[4], Y. Hong[4], S. Lowette[4], I. Makarenko[4], D. Müller[4], S. Tavernier[4], M. Tytgat[4,c], G.P. Van Onsem[4], S. Van Putte[4], D. Vannerom[4], B. Bilin[5], B. Clerbaux[5], A.K. Das[5], I. De Bruyn[5], G. De Lentdecker[5], H. Evard[5], L. Favart[5], P. Gianneios[5], A. Khalilzadeh[5], F.A. Khan[5], A. Malara[5], M.A. Shahzad[5], L. Thomas[5], M. Vanden Bemden[5], C. Vander Velde[5], P. Vanlaer[5], F. Zhang[5], M. De Coen[6], D. Dobur[6], G. Gokbulut[6], J. Knolle[6], L. Lambrecht[6], D. Marckx[6], K. Skovpen[6], N. Van Den Bossche[6], J. van der Linden[6], J. Vandenbroeck[6], L. Wezenbeek[6], S. Bein[7], A. Benecke[7], A. Bethani[7], G. Bruno[7], A. Cappati[7], J. De Favereau De Jeneret[7], C. Delaere[7], A. Giammanco[7], A.O. Guzel[7], Sa. Jain[7], V. Lemaitre[7], J. Lidrych[7], P. Mastrapasqua[7], S. Turkcapar[7], G.A. Alves[8], E. Coelho[8], G. Correia Silva[8], C. Hensel[8], T. Menezes De Oliveira[8], C. Mora Herrera[8,d], P. Rebello Teles[8], M. Soeiro[8], E.J. Tonelli Manganote[8,e], A. Vilela Pereira[8,d], W.L. Aldá Júnior[9], M. Barroso Ferreira Filho[9], H. Brandao Malbouisson[9], W. Carvalho[9], J. Chinellato[9,f], E.M. Da Costa[9], G.G. Da Silveira[9,g], D. De Jesus Damiao[9], S. Fonseca De Souza[9], R. Gomes De Souza[9], T. Laux Kuhn[9,g], M. Macedo[9], K. Mota Amarilo[9], L. Mundim[9], H. Nogima[9], J.P. Pinheiro[9], A. Santoro[9], A. Sznajder[9], M. Thiel[9], C.A. Bernardes[10,g], L. Calligaris[10], E.M. Gregores[10], I. Maietto Silverio[10], P.G. Mercadante[10], S.F. Novaes[10], B. Orzari[10], Sandra S. Padula[10], V. Scheurer[10], T.R. Fernandez Perez Tomei[10], A. Aleksandrov[11], G. Antchev[11], R. Hadjiiska[11], P. Iaydjiev[11], M. Misheva[11], M. Shopova[11], G. Sultanov[11], A. Dimitrov[12], L. Litov[12], B. Pavlov[12], P. Petkov[12], A. Petrov[12], E. Shumka[12], S. Keshri[13], D. Laroze[13], S. Thakur[13], T. Cheng[14], T. Javaid[14], L. Yuan[14], Z. Hu[15], Z. Liang[15], J. Liu[15], G.M. Chen[16,h], H.S. Chen[16,h], M. Chen[16,h], Q. Hou[16], F. Iemmi[16], C.H. Jiang[16], A. Kapoor[16,i], H. Liao[16], Z.-A. Liu[16,j], R. Sharma[16,k], J.N. Song[16,j], J. Tao[16], C. Wang[16,h], J. Wang[16], H. Zhang[16], J. Zhao[16], A. Agapitos[17], Y. Ban[17], A. Carvalho Antunes De Oliveira[17], S. Deng[17], B. Guo[17], C. Jiang[17], A. Levin[17], C. Li[17], Q. Li[17], Y. Mao[17], S. Qian[17], S.J. Qian[17], X. Qin[17], X. Sun[17], D. Wang[17], H. Yang[17], Y. Zhao[17], C. Zhou[17], S. Yang[18], Z. You[19], K. Jaffel[20], N. Lu[20], G. Bauer[21,l], B. Li[21,m], H. Wang[21], K. Yi[21,n], J. Zhang[21], Y. Li[22], Z. Lin[23], C. Lu[23], M. Xiao[23], C. Avila[24], D.A. Barbosa Trujillo[24], A. Cabrera[24], C. Florez[24], J. Fraga[24], J.A. Reyes Vega[24], J. Jaramillo[25], C. Rendón[25], M. Rodriguez[25], A.A. Ruales Barbosa[25], J.D. Ruiz Alvarez[25], D. Giljanovic[26], N. Godinovic[26], D. Lelas[26], A. Sculac[26], M. Kovac[27], A. Petkovic[27], T. Sculac[27], P. Bargassa[28], V. Brigljevic[28], B.K. Chitroda[28], D. Ferencek[28], K. Jakovcic[28], A. Starodumov[28], T. Susa[28], A. Attikis[29], K. Christoforou[29], A. Hadjiagapiou[29], C. Leonidou[29], J. Mousa[29], C. Nicolaou[29], L. Paizanos[29], F. Ptochos[29], P.A. Razis[29], H. Rykaczewski[29], H. Saka[29], A. Stepennov[29], M. Finger[30], M. Finger Jr.[30], A. Kveton[30], E. Ayala[31], E. Carrera Jarrin[32], A.A. Abdelalim[33,o,p], S. Elgammal[33,q], A. Ellithi Kamel[33,r],

JHEP05(2026)175

M.A. Mahmoud[34], M. Abdullah Al-Mashad[34], K. Ehataht[35], M. Kadastik[35], T. Lange[35], C. Nielsen[35], J. Pata[35], M. Raidal[35], L. Tani[35], C. Veelken[35], K. Osterberg[36], M. Voutilainen[36], N. Bin Norjoharuddeen[37], E. Brücken[37], F. Garcia[37], P. Inkaew[37], K.T.S. Kallonen[37], T. Lampén[37], K. Lassila-Perini[37], S. Lehti[37], T. Lindén[37], M. Myllymäki[37], M.m. Rantanen[37], J. Tuominiemi[37], H. Kirschenmann[38], P. Luukka[38], H. Petrow[38], M. Besancon[39], F. Couderc[39], M. Dejardin[39], D. Denegri[39], J.L. Faure[39], F. Ferri[39], S. Ganjour[39], P. Gras[39], G. Hamel de Monchenault[39], M. Kumar[39], V. Lohezic[39], J. Malcles[39], F. Orlandi[39], L. Portales[39], A. Rosowsky[39], M.Ö. Sahin[39], A. Savoy-Navarro[39,s], P. Simkina[39], M. Titov[39], M. Tornago[39], F. Beaudette[40], G. Boldrini[40], P. Busson[40], C. Charlot[40], M. Chiusi[40], T.D. Cuisset[40], F. Damas[40], O. Davignon[40], A. De Wit[40], I.T. Ehle[40], B.A. Fontana Santos Alves[40], S. Ghosh[40], A. Gilbert[40], R. Granier de Cassagnac[40], B. Harikrishnan[40], L. Kalipoliti[40], G. Liu[40], M. Manoni[40], M. Nguyen[40], S. Obraztsov[40], C. Ochando[40], R. Salerno[40], J.B. Sauvan[40], Y. Sirois[40], G. Sokmen[40], L. Urda Gómez[40], E. Vernazza[40], A. Zabi[40], A. Zghiche[40], J.-L. Agram[41,t], J. Andrea[41], D. Bloch[41], J.-M. Brom[41], E.C. Chabert[41], C. Collard[41], S. Falke[41], U. Goerlach[41], R. Haeberle[41], A.-C. Le Bihan[41], M. Meena[41], O. Poncet[41], G. Saha[41], M.A. Sessini[41], P. Van Hove[41], P. Vaucelle[41], A. Di Florio[42], D. Amram[43], S. Beauceron[43], B. Blancon[43], G. Boudoul[43], N. Chanon[43], D. Contardo[43], P. Depasse[43], C. Dozen[43,u], H. El Mamouni[43], J. Fay[43], S. Gascon[43], M. Gouzevitch[43], C. Greenberg[43], G. Grenier[43], B. Ille[43], E. Jourd'huy[43], I.B. Laktineh[43], M. Lethuillier[43], L. Mirabito[43], S. Perries[43], A. Purohit[43], M. Vander Donckt[43], P. Verdier[43], J. Xiao[43], I. Lomidze[44], T. Toriashvili[44,v], Z. Tsamalaidze[44,w], V. Botta[45], S. Consuegra Rodríguez[45], L. Feld[45], K. Klein[45], M. Lipinski[45], D. Meuser[45], P. Nattland[45], A. Pauls[45], D. Pérez Adán[45], N. Röwert[45], M. Teroerde[45], S. Diekmann[46], A. Dodonova[46], N. Eich[46], D. Eliseev[46], F. Engelke[46], J. Erdmann[46], M. Erdmann[46], B. Fischer[46], T. Hebbeker[46], K. Hoepfner[46], F. Ivone[46], A. Jung[46], N. Kumar[46], M.y. Lee[46], F. Mausolf[46], M. Merschmeyer[46], A. Meyer[46], F. Nowotny[46], A. Pozdnyakov[46], Y. Rath[46], W. Redjeb[46], F. Rehm[46], H. Reithler[46], V. Sarkisovi[46], A. Schmidt[46], C. Seth[46], A. Sharma[46], J.L. Spah[46], F. Torres Da Silva De Araujo[46,x], S. Wiedenbeck[46], S. Zaleski[46], C. Dziwok[47], G. Flügge[47], T. Kress[47], A. Nowack[47], O. Pooth[47], A. Stahl[47], T. Ziemons[47], A. Zotz[47], H. Aarup Petersen[48], M. Aldaya Martin[48], J. Alimena[48], S. Amoroso[48], Y. An[48], J. Bach[48], S. Baxter[48], M. Bayatmakou[48], H. Becerril Gonzalez[48], O. Behnke[48], A. Belvedere[48], F. Blekman[48,y], K. Borras[48,z], A. Campbell[48], A. Cardini[48], S. Chatterjee[48], F. Colombina[48], M. De Silva[48], G. Eckerlin[48], D. Eckstein[48], E. Gallo[48,y], A. Geiser[48], V. Guglielmi[48], M. Guthoff[48], A. Hinzmann[48], L. Jeppe[48], B. Kaech[48], M. Kasemann[48], C. Kleinwort[48], R. Kogler[48], M. Komm[48], D. Krücker[48], W. Lange[48], D. Leyva Pernia[48], K. Lipka[48,aa], W. Lohmann[48,ab], F. Lorkowski[48], R. Mankel[48], I.-A. Melzer-Pellmann[48], M. Mendizabal Morentin[48], A.B. Meyer[48], G. Milella[48], K. Moral Figueroa[48], A. Mussgiller[48], L.P. Nair[48], J. Niedziela[48], A. Nürnberg[48], J. Park[48], E. Ranken[48], A. Raspereza[48], D. Rastorguev[48], L. Rygaard[48], J. Rübenach[48], M. Scham[48,ac,ad], S. Schnake[48,z], C. Schwanenberger[48,y], P. Schütze[48], D. Selivanova[48], K. Sharko[48], M. Shchedrolosiev[48], D. Stafford[48], F. Vazzoler[48], A. Ventura Barroso[48], R. Walsh[48], D. Wang[48], Q. Wang[48], K. Wichmann[48], L. Wiens[48,z], C. Wissing[48],

JHEP05(2026)175

Y. Yang[48], S. Zakharov[48], A. Zimermmane Castro Santos[48], A. Albrecht[49], S. Albrecht[49], M. Antonello[49], S. Bollweg[49], M. Bonanomi[49], P. Connor[49], K. El Morabit[49], Y. Fischer[49], E. Garutti[49], A. Grohsjean[49], J. Haller[49], D. Hundhausen[49], H.R. Jabusch[49], G. Kasieczka[49], P. Keicher[49], R. Klanner[49], W. Korcari[49], T. Kramer[49], C.c. Kuo[49], V. Kutzner[49], F. Labe[49], J. Lange[49], A. Lobanov[49], C. Matthies[49], L. Moureaux[49], M. Mrowietz[49], A. Nigamova[49], K. Nikolopoulos[49], Y. Nissan[49], A. Paasch[49], K.J. Pena Rodriguez[49], T. Quadfasel[49], B. Raciti[49], M. Rieger[49], D. Savoiu[49], J. Schindler[49], P. Schleper[49], M. Schröder[49], J. Schwandt[49], M. Sommerhalder[49], H. Stadie[49], G. Steinbrück[49], A. Tews[49], B. Wiederspan[49], M. Wolf[49], S. Brommer[50], E. Butz[50], Y.M. Chen[50], T. Chwalek[50], A. Dierlamm[50], G.G. Dincer[50], U. Elicabuk[50], N. Faltermann[50], M. Giffels[50], A. Gottmann[50], F. Hartmann[50,ae], R. Hofsaess[50], M. Horzela[50], U. Husemann[50], J. Kieseler[50], M. Klute[50], O. Lavoryk[50], J.M. Lawhorn[50], M. Link[50], A. Lintuluoto[50], S. Maier[50], M. Mormile[50], Th. Müller[50], M. Neukum[50], M. Oh[50], E. Pfeffer[50], M. Presilla[50], G. Quast[50], K. Rabbertz[50], B. Regnery[50], R. Schmieder[50], N. Shadskiy[50], I. Shvetsov[50], H.J. Simonis[50], L. Sowa[50], L. Stockmeier[50], K. Tauqeer[50], M. Toms[50], B. Topko[50], N. Trevisani[50], T. Voigtländer[50], R.F. Von Cube[50], J. Von Den Driesch[50], M. Wassmer[50], S. Wieland[50], F. Wittig[50], R. Wolf[50], X. Zuo[50], G. Anagnostou[51], G. Daskalakis[51], A. Kyriakis[51], A. Papadopoulos[51,ae], A. Stakia[51], G. Melachroinos[52], Z. Painesis[52], I. Paraskevas[52], N. Saoulidou[52], K. Theofilatos[52], E. Tziaferi[52], K. Vellidis[52], I. Zisopoulos[52], T. Chatzistavrou[53], G. Karapostoli[53], K. Kousouris[53], E. Siamarkou[53], G. Tsipolitis[53], I. Bestintzanos[54], I. Evangelou[54], C. Foudas[54], C. Kamtsikis[54], P. Katsoulis[54], P. Kokkas[54], P.G. Kosmoglou Kioseoglou[54], N. Manthos[54], I. Papadopoulos[54], J. Strologas[54], C. Hajdu[55], D. Horvath[55,af,ag], K. Márton[55], A.J. Rádl[55,ah], F. Sikler[55], V. Veszpremi[55], M. Csanád[56], K. Farkas[56], A. Fehérkuti[56,ai], M.M.A. Gadallah[56,aj], Á. Kadlecsik[56], G. Pásztor[56], G.I. Veres[56], B. Ujvari[57], G. Zilizi[57], G. Bencze[58], S. Czellar[58], J. Molnar[58], Z. Szillasi[58], T. Csorgo[59,ai], F. Nemes[59,ai], T. Novak[59], S. Bansal[60], S.B. Beri[60], V. Bhatnagar[60], G. Chaudhary[60], S. Chauhan[60], N. Dhingra[60,ak], A. Kaur[60], A. Kaur[60], H. Kaur[60], M. Kaur[60], S. Kumar[60], T. Sheokand[60], J.B. Singh[60], A. Singla[60], A. Bhardwaj[61], A. Chhetri[61], B.C. Choudhary[61], A. Kumar[61], A. Kumar[61], M. Naimuddin[61], S. Saumya[61], K. Ranjan[61], M.K. Saini[61], S. Mukherjee[62], S. Baradia[63], S. Barman[63,al], S. Bhattacharya[63], S. Das Gupta[63], S. Dutta[63], S. Dutta[63], S. Sarkar[63], M.M. Ameen[64], P.K. Behera[64], S.C. Behera[64], S. Chatterjee[64], G. Dash[64], A. Dattamunsi[64], P. Jana[64], P. Kalbhor[64], S. Kamble[64], J.R. Komaragiri[64,am], D. Kumar[64,am], T. Mishra[64], B. Parida[64,an], P.R. Pujahari[64], N.R. Saha[64], A.K. Sikdar[64], R.K. Singh[64], P. Verma[64], S. Verma[64], A. Vijay[64], S. Dugad[65], G.B. Mohanty[65], M. Shelake[65], P. Suryadevara[65], A. Bala[66], S. Banerjee[66], S. Bhowmik[66,ao], R.M. Chatterjee[66], M. Guchait[66], Sh. Jain[66], A. Jaiswal[66], B.M. Joshi[66], S. Kumar[66], G. Majumder[66], K. Mazumdar[66], S. Parolia[66], A. Thachayath[66], S. Bahinipati[67,ap], C. Kar[67], D. Maity[67,aq], P. Mal[67], K. Naskar[67,aq], A. Nayak[67,aq], S. Nayak[67], K. Pal[67], R. Raturi[67], P. Sadangi[67], S.K. Swain[67], S. Varghese[67,aq], D. Vats[67,aq], S. Acharya[68,ar], A. Alpana[68], S. Dube[68], B. Gomber[68,ar], P. Hazarika[68], B. Kansal[68], A. Laha[68], B. Sahu[68,ar], S. Sharma[68], K.Y. Vaish[68], H. Bakhshiansohi[69,as], A. Jafari[69,at], M. Zeinali[69,au], S. Bashiri[70], S. Chenarani[70,av], S.M. Etesami[70],

JHEP05(2026)175

Y. Hosseini[70], M. Khakzad[70], E. Khazaie[70], M. Mohammadi Najafabadi[70], S. Tizchang[70,aw], M. Felcini[71], M. Grunewald[71], M. Abbrescia[72a,72b], M. Buonsante[72a,72b], A. Colaleo[72a,72b], D. Creanza[72a,72c], B. D'Anzi[72a,72b], N. De Filippis[72a,72c], M. De Palma[72a,72b], W. Elmetenawee[72a,72b,o], N. Ferrara[72a,72b], L. Fiore[72a], G. Iaselli[72a,72c], L. Longo[72a], M. Louka[72a,72b], G. Maggi[72a,72c], M. Maggi[72a], I. Margjeka[72a], V. Mastrapasqua[72a,72b], S. My[72a,72b], S. Nuzzo[72a,72b], A. Pellecchia[72a,72b], A. Pompili[72a,72b], G. Pugliese[72a,72c], R. Radogna[72a,72b], D. Ramos[72a], A. Ranieri[72a], L. Silvestris[72a], F.M. Simone[72a,72c], A. Stamerra[72a,72b], Ü. Sözbilir[72a], D. Troiano[72a,72b], R. Venditti[72a,72b], P. Verwilligen[72a], A. Zaza[72a,72b], G. Abbiendi[73a], C. Battilana[73a,73b], D. Bonacorsi[73a,73b], P. Capiluppi[73a,73b], A. Castro[73a,73b,†], F.R. Cavallo[73a], M. Cuffiani[73a,73b], G.M. Dallavalle[73a], T. Diotalevi[73a,73b], F. Fabbri[73a], A. Fanfani[73a,73b], D. Fasanella[73a], P. Giacomelli[73a], L. Giommi[73a,73b], C. Grandi[73a], L. Guiducci[73a,73b], S. Lo Meo[73a,ax], M. Lorusso[73a,73b], L. Lunerti[73a], S. Marcellini[73a], G. Masetti[73a], F.L. Navarria[73a,73b], G. Paggi[73a,73b], A. Perrotta[73a], F. Primavera[73a,73b], A.M. Rossi[73a,73b], S. Rossi Tisbeni[73a,73b], T. Rovelli[73a,73b], G.P. Siroli[73a,73b], S. Costa[74a,74b,ay], A. Di Mattia[74a], A. Lapertosa[74a], R. Potenza[74a,74b], A. Tricomi[74a,74b,ay], P. Assiouras[75a], G. Barbagli[75a], G. Bardelli[75a,75b], M. Bartolini[75a,75b], B. Camaiani[75a,75b], A. Cassese[75a], R. Ceccarelli[75a], V. Ciulli[75a,75b], C. Civinini[75a], R. D'Alessandro[75a,75b], L. Damenti[75a,75b], E. Focardi[75a,75b], T. Kello[75a], G. Latino[75a,75b], P. Lenzi[75a,75b], M. Lizzo[75a], M. Meschini[75a], S. Paoletti[75a], A. Papanastassiou[75a,75b], G. Sguazzoni[75a], L. Viliani[75a], L. Benussi[76], S. Bianco[76], S. Meola[76,az], D. Piccolo[76], M. Alves Gallo Pereira[77a], F. Ferro[77a], E. Robutti[77a], S. Tosi[77a,77b], A. Benaglia[78a], F. Brivio[78a], F. Cetorelli[78a,78b], F. De Guio[78a,78b], M.E. Dinardo[78a,78b], P. Dini[78a], S. Gennai[78a], R. Gerosa[78a,78b], A. Ghezzi[78a,78b], P. Govoni[78a,78b], L. Guzzi[78a], G. Lavizzari[78a,78b], M.T. Lucchini[78a,78b], M. Malberti[78a], S. Malvezzi[78a], A. Massironi[78a], D. Menasce[78a], L. Moroni[78a], M. Paganoni[78a,78b], S. Palluotto[78a,78b], D. Pedrini[78a], A. Perego[78a,78b], B.S. Pinolini[78a], G. Pizzati[78a,78b], S. Ragazzi[78a,78b], T. Tabarelli de Fatis[78a,78b], S. Buontempo[79a], A. Cagnotta[79a,79b], F. Carnevali[79a,79b], N. Cavallo[79a,79c], F. Fabozzi[79a,79c], A.O.M. Iorio[79a,79b], L. Lista[79a,79b,ba], P. Paolucci[79a,ae], B. Rossi[79a], R. Ardino[80a], P. Azzi[80a], N. Bacchetta[80a,bb], D. Bisello[80a,80b], P. Bortignon[80a], G. Bortolato[80a,80b], A.C.M. Bulla[80a], R. Carlin[80a,80b], P. Checchia[80a], T. Dorigo[80a,bc], F. Fanzago[80a], U. Gasparini[80a,80b], S. Giorgetti[80a], E. Lusiani[80a], M. Margoni[80a,80b], A.T. Meneguzzo[80a,80b], J. Pazzini[80a,80b], P. Ronchese[80a,80b], R. Rossin[80a,80b], F. Simonetto[80a,80b], M. Tosi[80a,80b], A. Triossi[80a,80b], S. Ventura[80a], M. Zanetti[80a,80b], P. Zotto[80a,80b], A. Zucchetta[80a,80b], G. Zumerle[80a,80b], A. Braghieri[81a], S. Calzaferri[81a], D. Fiorina[81a], P. Montagna[81a,81b], M. Pelliccioni[81a], V. Re[81a], C. Riccardi[81a,81b], P. Salvini[81a], I. Vai[81a,81b], P. Vitulo[81a,81b], S. Ajmal[82a,82b], M.E. Ascioti[82a,82b], G.M. Bilei[82a], C. Carrivale[82a,82b], D. Ciangottini[82a,82b], L. Fanò[82a,82b], V. Mariani[82a,82b], M. Menichelli[82a], F. Moscatelli[82a,bd], A. Rossi[82a,82b], A. Santocchia[82a,82b], D. Spiga[82a], T. Tedeschi[82a,82b], C. Aimè[83a,83b], C.A. Alexe[83a,83c], P. Asenov[83a,83b], P. Azzurri[83a], G. Bagliesi[83a], R. Bhattacharya[83a], L. Bianchini[83a,83b], T. Boccali[83a], E. Bossini[83a], D. Bruschini[83a,83c], R. Castaldi[83a], F. Cattafesta[83a,83c], M.A. Ciocci[83a,83b], M. Cipriani[83a,83b], V. D'Amante[83a,83d], R. Dell'Orso[83a], S. Donato[83a,83b], A. Giassi[83a],

JHEP05(2026)175

F. Ligabue[83a,83c], A.C. Marini[83a,83b], D. Matos Figueiredo[83a], A. Messineo[83a,83b], S. Mishra[83a], V.K. Muraleedharan Nair Bindhu[83a,83b,aq], M. Musich[83a,83b], S. Nandan[83a], F. Palla[83a], A. Rizzi[83a,83b], G. Rolandi[83a,83c], S. Roy Chowdhury[83a,ao], T. Sarkar[83a], A. Scribano[83a], P. Spagnolo[83a], F. Tenchini[83a,83b], R. Tenchini[83a], G. Tonelli[83a,83b], N. Turini[83a,83d], F. Vaselli[83a,83c], A. Venturi[83a], P.G. Verdini[83a], P. Akrap[84a,84b], C. Basile[84a,84b], F. Cavallari[84a], L. Cunqueiro Mendez[84a,84b], D. Del Re[84a,84b], E. Di Marco[84a,84b], M. Diemoz[84a], F. Errico[84a,84b], R. Gargiulo[84a,84b], E. Longo[84a,84b], L. Martikainen[84a,84b], J. Mijuskovic[84a,84b], G. Organtini[84a,84b], N. Palmeri[84a,84b], F. Pandolfi[84a], R. Paramatti[84a,84b], C. Quaranta[84a,84b], S. Rahatlou[84a,84b], C. Rovelli[84a], F. Santanastasio[84a,84b], L. Soffi[84a], V. Vladimirov[84a,84b], N. Amapane[85a,85b], R. Arcidiacono[85a,85c], S. Argiro[85a,85b], M. Arneodo[85a,85c], N. Bartosik[85a,85c], R. Bellan[85a,85b], C. Biino[85a], C. Borca[85a,85b], N. Cartiglia[85a], M. Costa[85a,85b], R. Covarelli[85a,85b], P. De Remigis[85a], N. Demaria[85a], L. Finco[85a], M. Grippo[85a,85b], B. Kiani[85a,85b], F. Legger[85a], F. Luongo[85a,85b], C. Mariotti[85a], L. Markovic[85a,85b], S. Maselli[85a], A. Mecca[85a,85b], L. Menzio[85a,85b], P. Meridiani[85a], E. Migliore[85a,85b], M. Monteno[85a], R. Mulargia[85a], M.M. Obertino[85a,85b], G. Ortona[85a], L. Pacher[85a,85b], N. Pastrone[85a], M. Ruspa[85a,85c], F. Siviero[85a,85b], V. Sola[85a,85b], A. Solano[85a,85b], C. Tarricone[85a,85b], D. Trocino[85a], G. Umoret[85a,85b], R. White[85a,85b], J. Babbar[86a,86b], S. Belforte[86a], V. Candelise[86a,86b], M. Casarsa[86a], F. Cossutti[86a], K. De Leo[86a], G. Della Ricca[86a,86b], S. Dogra[87], J. Hong[87], J. Kim[87], D. Lee[87], H. Lee[87], S.W. Lee[87], C.S. Moon[87], Y.D. Oh[87], M.S. Ryu[87], S. Sekmen[87], B. Tae[87], Y.C. Yang[87], M.S. Kim[88], G. Bak[89], P. Gwak[89], H. Kim[89], D.H. Moon[89], E. Asilar[90], J. Choi[90,be], D. Kim[90], T.J. Kim[90], J.A. Merlin[90], Y. Ryou[90], S. Choi[91], S. Han[91], B. Hong[91], K. Lee[91], K.S. Lee[91], S. Lee[91], J. Yoo[91], J. Goh[92], S. Yang[92], Y. Kang[93], H. S. Kim[93], Y. Kim[93], S. Lee[93], J. Almond[94], J.H. Bhyun[94], J. Choi[94], J. Choi[94], W. Jun[94], J. Kim[94], Y.W. Kim[94], S. Ko[94], H. Lee[94], J. Lee[94], J. Lee[94], B.H. Oh[94], S.B. Oh[94], H. Seo[94], U.K. Yang[94], I. Yoon[94], W. Jang[95], D.Y. Kang[95], S. Kim[95], B. Ko[95], J.S.H. Lee[95], Y. Lee[95], I.C. Park[95], Y. Roh[95], I.J. Watson[95], S. Ha[96], K. Hwang[96], B. Kim[96], K. Lee[96], H.D. Yoo[96], M. Choi[97], M.R. Kim[97], H. Lee[97], Y. Lee[97], I. Yu[97], T. Beyrouthy[98], Y. Gharbia[98], F. Alazemi[99], K. Dreimanis[100], A. Gaile[100], C. Munoz Diaz[100], D. Osite[100], G. Pikurs[100], A. Potrebko[100], M. Seidel[100], D. Sidiropoulos Kontos[100], N.R. Strautnieks[101], M. Ambrozas[102], A. Juodagalvis[102], A. Rinkevicius[102], G. Tamulaitis[102], I. Yusuff[103,bf], Z. Zolkapli[103], J.F. Benitez[104], A. Castaneda Hernandez[104], H.A. Encinas Acosta[104], L.G. Gallegos Maríñez[104], M. León Coello[104], J.A. Murillo Quijada[104], A. Sehrawat[104], L. Valencia Palomo[104], G. Ayala[105], H. Castilla-Valdez[105], H. Crotte Ledesma[105], E. De La Cruz-Burelo[105], I. Heredia-De La Cruz[105,bg], R. Lopez-Fernandez[105], J. Mejia Guisao[105], A. Sánchez Hernández[105], C. Oropeza Barrera[106], D.L. Ramirez Guadarrama[106], M. Ramírez García[106], I. Bautista[107], F.E. Neri Huerta[107], I. Pedraza[107], H.A. Salazar Ibarguen[107], C. Uribe Estrada[107], I. Bubanja[108], N. Raicevic[108], P.H. Butler[109], A. Ahmad[110], M.I. Asghar[110], A. Awais[110], M.I.M. Awan[110], H.R. Hoorani[110], W.A. Khan[110], V. Avati[111], A. Bellora[111,bh], L. Forthomme[111], L. Grzanka[111], M. Malawski[111], K. Piotrzkowski[111], H. Bialkowska[112], M. Bluj[112],

JHEP05(2026)175

M. Górski[112], M. Kazana[112], M. Szleper[112], P. Zalewski[112], K. Bunkowski[113], K. Doroba[113], A. Kalinowski[113], M. Konecki[113], J. Krolikowski[113], A. Muhammad[113], P. Fokow[114], K. Pozniak[114], W. Zabolotny[114], M. Araujo[115], D. Bastos[115], C. Beirão Da Cruz E Silva[115], A. Boletti[115], M. Bozzo[115], T. Camporesi[115], G. Da Molin[115], P. Faccioli[115], M. Gallinaro[115], J. Hollar[115], N. Leonardo[115], G.B. Marozzo[115], A. Petrilli[115], M. Pisano[115], J. Seixas[115], J. Varela[115], J.W. Wulff[115], P. Adzic[116], P. Milenovic[116], D. Devetak[117], M. Dordevic[117], J. Milosevic[117], L. Nadderd[117], V. Rekovic[117], M. Stojanovic[117], J. Alcaraz Maestre[118], J.A. Brochero Cifuentes[118], M. Cepeda[118], M. Cerrada[118], N. Colino[118], B. De La Cruz[118], A. Delgado Peris[118], A. Escalante Del Valle[118], Cristina F. Bedoya[118], D. Fernández Del Val[118], J.P. Fernández Ramos[118], J. Flix[118], M.C. Fouz[118], O. Gonzalez Lopez[118], S. Goy Lopez[118], J.M. Hernandez[118], M.I. Josa[118], J. Llorente Merino[118], Oliver M. Carretero[118], C. Martin Perez[118], E. Martin Viscasillas[118], D. Moran[118], C. M. Morcillo Perez[118], Á. Navarro Tobar[118], C. Perez Dengra[118], J. Puerta Pelayo[118], A. Pérez-Calero Yzquierdo[118], I. Redondo[118], J. Sastre[118], J. Vazquez Escobar[118], J.F. de Trocóniz[119], B. Alvarez Gonzalez[120], J. Cuevas[120], J. Fernandez Menendez[120], S. Folgueras[120], I. Gonzalez Caballero[120], P. Leguina[120], E. Palencia Cortezon[120], J. Prado Pico[120], V. Rodríguez Bouza[120], A. Soto Rodríguez[120], A. Trapote[120], C. Vico Villalba[120], P. Vischia[120], S. Blanco Fernández[121], I.J. Cabrillo[121], A. Calderon[121], J. Duarte Campderros[121], M. Fernandez[121], G. Gomez[121], C. Lasaosa García[121], R. Lopez Ruiz[121], C. Martinez Rivero[121], P. Martinez Ruiz del Arbol[121], F. Matorras[121], P. Matorras Cuevas[121], E. Navarrete Ramos[121], J. Piedra Gomez[121], L. Scodellaro[121], I. Vila[121], J.M. Vizan Garcia[121], D.D.C. Wickramarathna[122], B. Kailasapathy[122,bi], W.G.D. Dharmaratna[123,bj], K. Liyanage[123], N. Perera[123], D. Abbaneo[124], C. Amendola[124], E. Auffray[124], J. Baechler[124], D. Barney[124], A. Bermúdez Martínez[124], M. Bianco[124], A.A. Bin Anuar[124], A. Bocci[124], L. Borgonovi[124], C. Botta[124], A. Bragagnolo[124], E. Brondolin[124], C.E. Brown[124], C. Caillol[124], G. Cerminara[124], N. Chernyavskaya[124], D. d'Enterria[124], A. Dabrowski[124], A. David[124], A. De Roeck[124], M.M. Defranchis[124], M. Deile[124], M. Dobson[124], W. Funk[124], S. Giani[124], D. Gigi[124], K. Gill[124], F. Glege[124], M. Glowacki[124], J. Hegeman[124], J.K. Heikkilä[124], B. Huber[124], V. Innocente[124], T. James[124], P. Janot[124], O. Kaluzinska[124], O. Karacheban[124,ab], G. Karathanasis[124], S. Laurila[124], P. Lecoq[124], E. Leutgeb[124], C. Lourenço[124], M. Magherini[124], L. Malgeri[124], M. Mannelli[124], M. Matthewman[124], A. Mehta[124], F. Meijers[124], S. Mersi[124], E. Meschi[124], M. Migliorini[124], V. Milosevic[124], F. Monti[124], F. Moortgat[124], M. Mulders[124], I. Neutelings[124], S. Orfanelli[124], F. Pantaleo[124], G. Petrucciani[124], A. Pfeiffer[124], M. Pierini[124], M. Pitt[124], H. Qu[124], D. Rabady[124], B. Ribeiro Lopes[124], F. Riti[124], M. Rovere[124], H. Sakulin[124], R. Salvatico[124], S. Sanchez Cruz[124], S. Scarfi[124], M. Selvaggi[124], A. Sharma[124], K. Shchelina[124], P. Silva[124], P. Sphicas[124,bk], A.G. Stahl Leiton[124], A. Steen[124], S. Summers[124], D. Treille[124], P. Tropea[124], D. Walter[124], J. Wanczyk[124,bl], J. Wang[124], S. Wuchterl[124], P. Zehetner[124], P. Zejdl[124], W.D. Zeuner[124], T. Bevilacqua[125,bm], L. Caminada[125,bm], A. Ebrahimi[125], W. Erdmann[125], R. Horisberger[125], Q. Ingram[125], H.C. Kaestli[125], D. Kotlinski[125],

JHEP05(2026)175

C. Lange[125], M. Missiroli[125,bm], L. Noehte[125,bm], T. Rohe[125], A. Samalan[125], T.K. Aarrestad[126], M. Backhaus[126], G. Bonomelli[126], A. Calandri[126], C. Cazzaniga[126], K. Datta[126], P. De Bryas Dexmiers D'archiac[126,bl], A. De Cosa[126], G. Dissertori[126], M. Dittmar[126], M. Donegà[126], F. Eble[126], M. Galli[126], K. Gedia[126], F. Glessgen[126], C. Grab[126], T.G. Harte[126], D. Hits[126], N. Härringer[126], W. Lustermann[126], A.-M. Lyon[126], R.A. Manzoni[126], M. Marchegiani[126], L. Marchese[126], A. Mascellani[126,bl], F. Nessi-Tedaldi[126], F. Pauss[126], V. Perovic[126], S. Pigazzini[126], B. Ristic[126], R. Seidita[126], J. Steggemann[126,bl], A. Tarabini[126], D. Valsecchi[126], R. Wallny[126], C. Amsler[127,bn], P. Bärtschi[127], M.F. Canelli[127], K. Cormier[127], M. Huwiler[127], W. Jin[127], A. Jofrehei[127], B. Kilminster[127], S. Leontsinis[127], S.P. Liechti[127], A. Macchiolo[127], P. Meiring[127], F. Meng[127], J. Motta[127], A. Reimers[127], P. Robmann[127], M. Senger[127], E. Shokr[127], F. Stäger[127], R. Tramontano[127], C. Adloff[128,bo], D. Bhowmik[128], C.M. Kuo[128], W. Lin[128], P.K. Rout[128], P.C. Tiwari[128,am], L. Ceard[129], K.F. Chen[129], Z.g. Chen[129], A. De Iorio[129], W.-S. Hou[129], T.h. Hsu[129], Y.w. Kao[129], S. Karmakar[129], G. Kole[129], Y.y. Li[129], R.-S. Lu[129], E. Paganis[129], X.f. Su[129], J. Thomas-Wilsker[129], L.s. Tsai[129], D. Tsionou[129], H.y. Wu[129], E. Yazgan[129], C. Asawatangtrakuldee[130], N. Srimanobhas[130], V. Wachirapusitanand[130], Y. Maghrbi[131], D. Agyel[132], F. Boran[132], F. Dolek[132], I. Dumanoglu[132,bp], E. Eskut[132], Y. Guler[132,bq], E. Gurpinar Guler[132,bq], C. Isik[132], O. Kara[132], A. Kayis Topaksu[132], Y. Komurcu[132], G. Onengut[132], K. Ozdemir[132,br], A. Polatoz[132], B. Tali[132,bs], U.G. Tok[132], E. Uslan[132], I.S. Zorbakir[132], M. Yalvac[133,bt], B. Akgun[134], I.O. Atakisi[134], E. Gülmez[134], M. Kaya[134,bu], O. Kaya[134,bv], S. Tekten[134,bw], A. Cakir[135], K. Cankocak[135,bp,bx], S. Sen[135,by], O. Aydilek[136,bz], B. Hacisahinoglu[136], I. Hos[136,ca], B. Kaynak[136], S. Ozkorucuklu[136], O. Potok[136], H. Sert[136], C. Simsek[136], C. Zorbilmez[136], S. Cerci[137], B. Isildak[137,cb], D. Sunar Cerci[137], T. Yetkin[137], A. Boyaryntsev[138], B. Grynyov[138], L. Levchuk[139], D. Anthony[140], J.J. Brooke[140], A. Bundock[140], F. Bury[140], E. Clement[140], D. Cussans[140], H. Flacher[140], J. Goldstein[140], H.F. Heath[140], M.-L. Holmberg[140], L. Kreczko[140], S. Paramesvaran[140], L. Robertshaw[140], V.J. Smith[140], K. Walkingshaw Pass[140], A.H. Ball[141], K.W. Bell[141], A. Belyaev[141,cc], C. Brew[141], R.M. Brown[141], D.J.A. Cockerill[141], C. Cooke[141], A. Elliot[141], K.V. Ellis[141], K. Harder[141], S. Harper[141], J. Linacre[141], K. Manolopoulos[141], D.M. Newbold[141], E. Olaiya[141], D. Petyt[141], T. Reis[141], A.R. Sahasransu[141], G. Salvi[141], T. Schuh[141], C.H. Shepherd-Themistocleous[141], I.R. Tomalin[141], K.C. Whalen[141], T. Williams[141], I. Andreou[142], R. Bainbridge[142], P. Bloch[142], O. Buchmuller[142], C.A. Carrillo Montoya[142], G.S. Chahal[142,cd], D. Colling[142], J.S. Dancu[142], I. Das[142], P. Dauncey[142], G. Davies[142], M. Della Negra[142], S. Fayer[142], G. Fedi[142], G. Hall[142], A. Howard[142], G. Iles[142], C.R. Knight[142], P. Krueper[142], J. Langford[142], K.H. Law[142], J. León Holgado[142], L. Lyons[142], A.-M. Magnan[142], B. Maier[142], S. Mallios[142], M. Mieskolainen[142], J. Nash[142,ce], M. Pesaresi[142], P.B. Pradeep[142], B.C. Radburn-Smith[142], A. Richards[142], A. Rose[142], L. Russell[142], K. Savva[142], C. Seez[142], R. Shukla[142], A. Tapper[142], K. Uchida[142], G.P. Uttley[142], T. Virdee[142,ae], M. Vojinovic[142], N. Wardle[142], D. Winterbottom[142], J.E. Cole[143], A. Khan[143], P. Kyberd[143], I.D. Reid[143], S. Abdullin[144], A. Brinkerhoff[144], E. Collins[144], M.R. Darwish[144], J. Dittmann[144], K. Hatakeyama[144], V. Hegde[144], J. Hiltbrand[144],

JHEP05(2026)175

B. McMaster[144], J. Samudio[144], S. Sawant[144], C. Sutantawibul[144], J. Wilson[144], R. Bartek[145], A. Dominguez[145], A.E. Simsek[145], S.S. Yu[145], B. Bam[146], A. Buchot Perraguin[146], R. Chudasama[146], S.I. Cooper[146], C. Crovella[146], S.V. Gleyzer[146], E. Pearson[146], C.U. Perez[146], P. Rumerio[146,cf], E. Usai[146], R. Yi[146], G. De Castro[147], Z. Demiragli[147], C. Erice[147], C. Fangmeier[147], C. Fernandez Madrazo[147], E. Fontanesi[147], D. Gastler[147], F. Golf[147], S. Jeon[147], J. O'cain[147], I. Reed[147], J. Rohlf[147], K. Salyer[147], D. Sperka[147], D. Spitzbart[147], I. Suarez[147], A. Tsatsos[147], A.G. Zecchinelli[147], G. Barone[148], G. Benelli[148], D. Cutts[148], S. Ellis[148], L. Gouskos[148], M. Hadley[148], U. Heintz[148], K.W. Ho[148], J.M. Hogan[148,cg], T. Kwon[148], G. Landsberg[148], K.T. Lau[148], J. Luo[148], S. Mondal[148], T. Russell[148], S. Sagir[148,ch], X. Shen[148], M. Stamenkovic[148], N. Venkatasubramanian[148], S. Abbott[149], B. Barton[149], C. Brainerd[149], R. Breedon[149], H. Cai[149], M. Calderon De La Barca Sanchez[149], M. Chertok[149], M. Citron[149], J. Conway[149], P.T. Cox[149], R. Erbacher[149], F. Jensen[149], O. Kukral[149], G. Mocellin[149], M. Mulhearn[149], S. Ostrom[149], W. Wei[149], S. Yoo[149], K. Adamidis[150], M. Bachtis[150], D. Campos[150], R. Cousins[150], A. Datta[150], G. Flores Avila[150], J. Hauser[150], M. Ignatenko[150], M.A. Iqbal[150], T. Lam[150], Y.f. Lo[150], E. Manca[150], A. Nunez Del Prado[150], D. Saltzberg[150], V. Valuev[150], R. Clare[151], J.W. Gary[151], G. Hanson[151], A. Aportela[152], A. Arora[152], J.G. Branson[152], S. Cittolin[152], S. Cooperstein[152], D. Diaz[152], J. Duarte[152], L. Giannini[152], Y. Gu[152], J. Guiang[152], R. Kansal[152], V. Krutelyov[152], R. Lee[152], J. Letts[152], M. Masciovecchio[152], F. Mokhtar[152], S. Mukherjee[152], M. Pieri[152], D. Primosch[152], M. Quinnan[152], V. Sharma[152], M. Tadel[152], E. Vourliotis[152], F. Würthwein[152], Y. Xiang[152], A. Yagil[152], A. Barzdukas[153], L. Brennan[153], C. Campagnari[153], K. Downham[153], C. Grieco[153], M.M. Hussain[153], J. Incandela[153], J. Kim[153], A.J. Li[153], P. Masterson[153], H. Mei[153], J. Richman[153], S.N. Santpur[153], U. Sarica[153], R. Schmitz[153], F. Setti[153], J. Sheplock[153], D. Stuart[153], T.Á. Vámi[153], X. Yan[153], D. Zhang[153], A. Albert[154], S. Bhattacharya[154], A. Bornheim[154], O. Cerri[154], J. Mao[154], H.B. Newman[154], G. Reales Gutiérrez[154], M. Spiropulu[154], J.R. Vlimant[154], S. Xie[154], R.Y. Zhu[154], J. Alison[155], S. An[155], P. Bryant[155], M. Cremonesi[155], V. Dutta[155], T. Ferguson[155], T.A. Gómez Espinosa[155], A. Harilal[155], A. Kallil Tharayil[155], M. Kanemura[155], C. Liu[155], T. Mudholkar[155], S. Murthy[155], P. Palit[155], K. Park[155], M. Paulini[155], A. Roberts[155], A. Sanchez[155], W. Terrill[155], J.P. Cumalat[156], W.T. Ford[156], A. Hart[156], A. Hassani[156], N. Manganelli[156], J. Pearkes[156], C. Savard[156], N. Schonbeck[156], K. Stenson[156], K.A. Ulmer[156], S.R. Wagner[156], N. Zipper[156], D. Zuolo[156], J. Alexander[157], X. Chen[157], D.J. Cranshaw[157], J. Dickinson[157], J. Fan[157], X. Fan[157], J. Grassi[157], S. Hogan[157], P. Kotamnives[157], J. Monroy[157], G. Niendorf[157], M. Oshiro[157], J.R. Patterson[157], M. Reid[157], A. Ryd[157], J. Thom[157], P. Wittich[157], R. Zou[157], M. Albrow[158], M. Alyari[158], O. Amram[158], G. Apollinari[158], A. Apresyan[158], L.A.T. Bauerdick[158], D. Berry[158], J. Berryhill[158], P.C. Bhat[158], K. Burkett[158], J.N. Butler[158], A. Canepa[158], G.B. Cerati[158], H.W.K. Cheung[158], F. Chlebana[158], C. Cosby[158], G. Cummings[158], I. Dutta[158], V.D. Elvira[158], J. Freeman[158], A. Gandrakota[158], Z. Gecse[158], L. Gray[158], D. Green[158], A. Grummer[158], S. Grünendahl[158], D. Guerrero[158], O. Gutsche[158], R.M. Harris[158], T.C. Herwig[158], J. Hirschauer[158], B. Jayatilaka[158], S. Jindariani[158],

JHEP05(2026)175

M. Johnson[158], U. Joshi[158], T. Klijnsma[158], B. Klima[158], K.H.M. Kwok[158], S. Lammel[158], C. Lee[158], D. Lincoln[158], R. Lipton[158], T. Liu[158], K. Maeshima[158], D. Mason[158], P. McBride[158], P. Merkel[158], S. Mrenna[158], S. Nahn[158], J. Ngadiuba[158], D. Noonan[158], S. Norberg[158], V. Papadimitriou[158], N. Pastika[158], K. Pedro[158], C. Pena[158,ci], F. Ravera[158], A. Reinsvold Hall[158,cj], L. Ristori[158], M. Safdari[158], E. Sexton-Kennedy[158], N. Smith[158], A. Soha[158], L. Spiegel[158], S. Stoynev[158], J. Strait[158], L. Taylor[158], S. Tkaczyk[158], N.V. Tran[158], L. Uplegger[158], E.W. Vaandering[158], C. Wang[158], I. Zoi[158], C. Aruta[159], P. Avery[159], D. Bourilkov[159], P. Chang[159], V. Cherepanov[159], R.D. Field[159], C. Huh[159], E. Koenig[159], M. Kolosova[159], J. Konigsberg[159], A. Korytov[159], K. Matchev[159], N. Menendez[159], G. Mitselmakher[159], K. Mohrman[159], A. Muthirakalayil Madhu[159], N. Rawal[159], S. Rosenzweig[159], Y. Takahashi[159], J. Wang[159], T. Adams[160], A. Al Kadhim[160], A. Askew[160], S. Bower[160], R. Hashmi[160], R.S. Kim[160], S. Kim[160], T. Kolberg[160], G. Martinez[160], H. Prosper[160], P.R. Prova[160], M. Wulansatiti[160], R. Yohay[160], J. Zhang[160], B. Alsufyani[161], S. Butalla[161], S. Das[161], T. Elkafrawy[161,ck], M. Hohlmann[161], E. Yanes[161], M.R. Adams[162], A. Baty[162], C. Bennett[162], R. Cavanaugh[162], D. S. Lemos[162], R. Escobar Franco[162], O. Evdokimov[162], C.E. Gerber[162], H. Gupta[162], M. Hawksworth[162], A. Hingrajiya[162], D.J. Hofman[162], J.h. Lee[162], C. Mills[162], S. Nanda[162], B. Ozek[162], D. Pilipovic[162], R. Pradhan[162], E. Prifti[162], P. Roy[162], T. Roy[162], S. Rudrabhatla[162], N. Singh[162], M.B. Tonjes[162], N. Varelas[162], M.A. Wadud[162], Z. Ye[162], J. Yoo[162], M. Alhusseini[163], D. Blend[163], K. Dilsiz[163,cl], L. Emediato[163], G. Karaman[163], O.K. Köseyan[163], J.-P. Merlo[163], A. Mestvirishvili[163,cm], O. Neogi[163], H. Ogul[163,cn], Y. Onel[163], A. Penzo[163], C. Snyder[163], E. Tiras[163,co], B. Blumenfeld[164], L. Corcodilos[164], J. Davis[164], A.V. Gritsan[164], L. Kang[164], S. Kyriacou[164], P. Maksimovic[164], M. Roguljic[164], J. Roskes[164], S. Sekhar[164], M. Swartz[164], A. Abreu[165], L.F. Alcerro Alcerro[165], J. Anguiano[165], S. Arteaga Escatel[165], P. Baringer[165], A. Bean[165], Z. Flowers[165], D. Grove[165], J. King[165], G. Krintiras[165], M. Lazarovits[165], C. Le Mahieu[165], J. Marquez[165], M. Murray[165], M. Nickel[165], S. Popescu[165,cp], C. Rogan[165], C. Royon[165], S. Sanders[165], C. Smith[165], G. Wilson[165], B. Allmond[166], A. Ivanov[166], K. Kaadze[166], Y. Maravin[166], J. Natoli[166], R. Gujju Gurunadha[166], D. Roy[166], G. Sorrentino[166], A. Baden[167], A. Belloni[167], J. Bistany-riebman[167], S.C. Eno[167], N.J. Hadley[167], S. Jabeen[167], R.G. Kellogg[167], T. Koeth[167], B. Kronheim[167], S. Lascio[167], P. Major[167], A.C. Mignerey[167], S. Nabili[167], C. Palmer[167], C. Papageorgakis[167], M.M. Paranjpe[167], E. Popova[167,cq], A. Shevelev[167], L. Wang[167], L. Zhang[167], C. Baldenegro Barrera[168], J. Bendavid[168], S. Bright-Thonney[168], I.A. Cali[168], P.c. Chou[168], M. D'Alfonso[168], J. Eysermans[168], C. Freer[168], G. Gomez-Ceballos[168], M. Goncharov[168], G. Grosso[168], P. Harris[168], D. Hoang[168], D. Kovalskyi[168], J. Krupa[168], L. Lavezzo[168], Y.-J. Lee[168], K. Long[168], C. Mcginn[168], A. Novak[168], M.I. Park[168], C. Paus[168], C. Reissel[168], C. Roland[168], G. Roland[168], S. Rothman[168], G.S.F. Stephans[168], Z. Wang[168], B. Wyslouch[168], T. J. Yang[168], B. Crossman[169], C. Kapsiak[169], M. Krohn[169], D. Mahon[169], J. Mans[169], B. Marzocchi[169], M. Revering[169], R. Rusack[169], R. Saradhy[169], N. Strobbe[169], K. Bloom[170], D.R. Claes[170], G. Haza[170], J. Hossain[170], C. Joo[170], I. Kravchenko[170], A. Rohilla[170], J.E. Siado[170], W. Tabb[170], A. Vagnerini[170],

JHEP05(2026)175

A. Wightman[170], F. Yan[170], D. Yu[170], H. Bandyopadhyay[171], L. Hay[171], H.w. Hsia[171], I. Iashvili[171], A. Kalogeropoulos[171], A. Kharchilava[171], M. Morris[171], D. Nguyen[171], S. Rappoccio[171], H. Rejeb Sfar[171], A. Williams[171], P. Young[171], G. Alverson[172], E. Barberis[172], J. Bonilla[172], B. Bylsma[172], M. Campana[172], J. Dervan[172], Y. Haddad[172], Y. Han[172], I. Israr[172], A. Krishna[172], P. Levchenko[172], J. Li[172], M. Lu[172], R. Mccarthy[172], D.M. Morse[172], T. Orimoto[172], A. Parker[172], L. Skinnari[172], E. Tsai[172], D. Wood[172], S. Dittmer[173], K.A. Hahn[173], D. Li[173], Y. Liu[173], M. Mcginnis[173], Y. Miao[173], D.G. Monk[173], M.H. Schmitt[173], A. Taliercio[173], M. Velasco[173], G. Agarwal[174], R. Band[174], R. Bucci[174], S. Castells[174], A. Das[174], R. Goldouzian[174], M. Hildreth[174], K. Hurtado Anampa[174], T. Ivanov[174], C. Jessop[174], K. Lannon[174], J. Lawrence[174], N. Loukas[174], L. Lutton[174], J. Mariano[174], N. Marinelli[174], I. Mcalister[174], T. McCauley[174], C. Mcgrady[174], C. Moore[174], Y. Musienko[174,cr], H. Nelson[174], M. Osherson[174], A. Piccinelli[174], R. Ruchti[174], A. Townsend[174], Y. Wan[174], M. Wayne[174], H. Yockey[174], M. Zarucki[174], L. Zygala[174], A. Basnet[175], M. Carrigan[175], L.S. Durkin[175], C. Hill[175], M. Joyce[175], M. Nunez Ornelas[175], K. Wei[175], D.A. Wenzl[175], B.L. Winer[175], B. R. Yates[175], H. Bouchamaoui[176], K. Coldham[176], P. Das[176], G. Dezoort[176], P. Elmer[176], P. Fackeldey[176], A. Frankenthal[176], B. Greenberg[176], N. Haubrich[176], K. Kennedy[176], G. Kopp[176], S. Kwan[176], Y. Lai[176], D. Lange[176], A. Loeliger[176], D. Marlow[176], I. Ojalvo[176], J. Olsen[176], F. Simpson[176], D. Stickland[176], C. Tully[176], L.H. Vage[176], S. Malik[177], R. Sharma[177], A.S. Bakshi[178], S. Chandra[178], R. Chawla[178], A. Gu[178], L. Gutay[178], M. Jones[178], A.W. Jung[178], A. K. Virdi[178], M. Liu[178], G. Negro[178], N. Neumeister[178], G. Paspalaki[178], S. Piperov[178], J.F. Schulte[178], F. Wang[178], A. Wildridge[178], W. Xie[178], Y. Yao[178], J. Dolen[179], N. Parashar[179], A. Pathak[179], D. Acosta[180], A. Agrawal[180], T. Carnahan[180], K.M. Ecklund[180], P.J. Fernández Manteca[180], S. Freed[180], P. Gardner[180], F.J.M. Geurts[180], I. Krommydas[180], W. Li[180], J. Lin[180], O. Miguel Colin[180], B.P. Padley[180], R. Redjimi[180], J. Rotter[180], E. Yigitbasi[180], Y. Zhang[180], A. Bodek[181], P. de Barbaro[181], R. Demina[181], J.L. Dulemba[181], A. Garcia-Bellido[181], O. Hindrichs[181], A. Khukhunaishvili[181], N. Parmar[181], P. Parygin[181,cq], R. Taus[181], B. Chiarito[182], J.P. Chou[182], S.V. Clark[182], D. Gadkari[182], Y. Gershtein[182], E. Halkiadakis[182], C. Houghton[182], D. Jaroslawski[182], S. Konstantinou[182], I. Laflotte[182], A. Lath[182], J. Martins[182], R. Montalvo[182], K. Nash[182], M. Heindl[182], J. Reichert[182], P. Saha[182], S. Salur[182], S. Schnetzer[182], S. Somalwar[182], R. Stone[182], S.A. Thayil[182], S. Thomas[182], J. Vora[182], D. Ally[183], A.G. Delannoy[183], S. Fiorendi[183], S. Higginbotham[183], T. Holmes[183], A.R. Kanuganti[183], N. Karunarathna[183], L. Lee[183], E. Nibigira[183], S. Spanier[183], D. Aebi[184], M. Ahmad[184], T. Akhter[184], K. Androsov[184,bl], A. Bolshov[184], O. Bouhali[184,cs], R. Eusebi[184], J. Gilmore[184], T. Huang[184], T. Kamon[184,ct], H. Kim[184], S. Luo[184], R. Mueller[184], A. Safonov[184], N. Akchurin[185], J. Damgov[185], Y. Feng[185], N. Gogate[185], Y. Kazhykarim[185], K. Lamichhane[185], S.W. Lee[185], C. Madrid[185], A. Mankel[185], T. Peltola[185], I. Volobouev[185], E. Appelt[186], Y. Chen[186], S. Greene[186], A. Gurrola[186], W. Johns[186], R. Kunnawalkam Elayavalli[186], A. Melo[186], D. Rathjens[186], F. Romeo[186], P. Sheldon[186], S. Tuo[186], J. Velkovska[186], J. Viinikainen[186], B. Cardwell[187], H. Chung[187], B. Cox[187], J. Hakala[187], R. Hirosky[187], A. Ledovskoy[187], C. Mantilla[187],

JHEP05(2026)175

C. Neu[187], C. Ramón Álvarez[187], S. Bhattacharya[188], P.E. Karchin[188], A. Aravind[189], S. Banerjee[189], K. Black[189], T. Bose[189], E. Chavez[189], S. Dasu[189], P. Everaerts[189], C. Galloni[189], H. He[189], M. Herndon[189], A. Herve[189], C.K. Koraka[189], A. Lanaro[189], R. Loveless[189], A. Mallampalli[189], A. Mohammadi[189], S. Mondal[189], G. Parida[189], D. Pinna[189], L. Pétré[189], A. Savin[189], V. Shang[189], V. Sharma[189], W.H. Smith[189], D. Teague[189], H.F. Tsoi[189], W. Vetens[189], A. Warden[189], S. Afanasiev[190], V. Alexakhin[190], Yu. Andreev[190], T. Aushev[190], D. Budkouski[190], M. Danilov[190,cr], T. Dimova[190,cr], A. Ershov[190,cr], I. Golutvin[190,†], I. Gorbunov[190], A. Gribushin[190,cr], V. Karjavine[190], V. Klyukhin[190,cr], O. Kodolova[190,cu,cq], V. Korenkov[190], A. Kozyrev[190,cr], A. Lanev[190], A. Malakhov[190], V. Matveev[190,cr], A. Nikitenko[190,cv,cw], V. Palichik[190], V. Perelygin[190], S. Petrushanko[190,cr], O. Radchenko[190,cr], M. Savina[190], V. Shalaev[190], S. Shmatov[190], S. Shulha[190], Y. Skovpen[190,cr], V. Smirnov[190], O. Teryaev[190], I. Tlisova[190,cr], A. Toropin[190], N. Voytishin[190], B.S. Yuldashev[190,cx,†], A. Zarubin[190], I. Zhizhin[190], V. Andreev[191], M. Azarkin[191], A. Babaev[191], V. Blinov[191,cr], E. Boos[191], V. Borshch[191], V. Bunichev[191], R. Chistov[191,cr], A. Dermenev[191], D. Druzhkin[191], L. Dudko[191], G. Gavrilov[191], V. Gavrilov[191], S. Gninenko[191], V. Golovtcov[191], N. Golubev[191], Y. Ivanov[191], K. Ivanov[191], V. Kachanov[191], A. Karneyeu[191], V. Kim[191,cr], M. Kirakosyan[191], D. Kirpichnikov[191], M. Kirsanov[191], N. Krasnikov[191], N. Lychkovskaya[191], V. Murzin[191], V. Oreshkin[191], M. Perfilov[191], S. Polikarpov[191,cr], V. Popov[191], V. Savrin[191], S. Slabospitskii[191], D. Sosnov[191], V. Sulimov[191], A. Terkulov[191], L. Uvarov[191], A. Uzunian[191], A. Vorobyev[191,†], G. Vorotnikov[191], A. Zhokin[191]

[1] *Yerevan Physics Institute, Yerevan, Armenia*
[2] *Institut für Hochenergiephysik, Vienna, Austria*
[3] *Universiteit Antwerpen, Antwerpen, Belgium*
[4] *Vrije Universiteit Brussel, Brussel, Belgium*
[5] *Université Libre de Bruxelles, Bruxelles, Belgium*
[6] *Ghent University, Ghent, Belgium*
[7] *Université Catholique de Louvain, Louvain-la-Neuve, Belgium*
[8] *Centro Brasileiro de Pesquisas Fisicas, Rio de Janeiro, Brazil*
[9] *Universidade do Estado do Rio de Janeiro, Rio de Janeiro, Brazil*
[10] *Universidade Estadual Paulista, Universidade Federal do ABC, São Paulo, Brazil*
[11] *Institute for Nuclear Research and Nuclear Energy, Bulgarian Academy of Sciences, Sofia, Bulgaria*
[12] *University of Sofia, Sofia, Bulgaria*
[13] *Instituto De Alta Investigación, Universidad de Tarapacá, Casilla 7 D, Arica, Chile*
[14] *Beihang University, Beijing, China*
[15] *Department of Physics, Tsinghua University, Beijing, China*
[16] *Institute of High Energy Physics, Beijing, China*
[17] *State Key Laboratory of Nuclear Physics and Technology, Peking University, Beijing, China*
[18] *State Key Laboratory of Nuclear Physics and Technology, Institute of Quantum Matter, South China Normal University, Guangzhou, China*
[19] *Sun Yat-Sen University, Guangzhou, China*
[20] *University of Science and Technology of China, Hefei, China*
[21] *Nanjing Normal University, Nanjing, China*
[22] *Institute of Modern Physics and Key Laboratory of Nuclear Physics and Ion-beam Application (MOE) – Fudan University, Shanghai, China*
[23] *Zhejiang University, Hangzhou, Zhejiang, China*
[24] *Universidad de Los Andes, Bogota, Colombia*
[25] *Universidad de Antioquia, Medellin, Colombia*

JHEP05(2026)175

[26] University of Split, Faculty of Electrical Engineering, Mechanical Engineering and Naval Architecture, Split, Croatia
[27] University of Split, Faculty of Science, Split, Croatia
[28] Institute Rudjer Boskovic, Zagreb, Croatia
[29] University of Cyprus, Nicosia, Cyprus
[30] Charles University, Prague, Czech Republic
[31] Escuela Politecnica Nacional, Quito, Ecuador
[32] Universidad San Francisco de Quito, Quito, Ecuador
[33] Academy of Scientific Research and Technology of the Arab Republic of Egypt, Egyptian Network of High Energy Physics, Cairo, Egypt
[34] Center for High Energy Physics (CHEP-FU), Fayoum University, El-Fayoum, Egypt
[35] National Institute of Chemical Physics and Biophysics, Tallinn, Estonia
[36] Department of Physics, University of Helsinki, Helsinki, Finland
[37] Helsinki Institute of Physics, Helsinki, Finland
[38] Lappeenranta-Lahti University of Technology, Lappeenranta, Finland
[39] IRFU, CEA, Université Paris-Saclay, Gif-sur-Yvette, France
[40] Laboratoire Leprince-Ringuet, CNRS/IN2P3, Ecole Polytechnique, Institut Polytechnique de Paris, Palaiseau, France
[41] Université de Strasbourg, CNRS, IPHC UMR 7178, Strasbourg, France
[42] Centre de Calcul de l'Institut National de Physique Nucleaire et de Physique des Particules, CNRS/IN2P3, Villeurbanne, France
[43] Institut de Physique des 2 Infinis de Lyon (IP2I), Villeurbanne, France
[44] Georgian Technical University, Tbilisi, Georgia
[45] RWTH Aachen University, I. Physikalisches Institut, Aachen, Germany
[46] RWTH Aachen University, III. Physikalisches Institut A, Aachen, Germany
[47] RWTH Aachen University, III. Physikalisches Institut B, Aachen, Germany
[48] Deutsches Elektronen-Synchrotron, Hamburg, Germany
[49] University of Hamburg, Hamburg, Germany
[50] Karlsruher Institut fuer Technologie, Karlsruhe, Germany
[51] Institute of Nuclear and Particle Physics (INPP), NCSR Demokritos, Aghia Paraskevi, Greece
[52] National and Kapodistrian University of Athens, Athens, Greece
[53] National Technical University of Athens, Athens, Greece
[54] University of Ioánnina, Ioánnina, Greece
[55] HUN-REN Wigner Research Centre for Physics, Budapest, Hungary
[56] MTA-ELTE Lendület CMS Particle and Nuclear Physics Group, Eötvös Loránd University, Budapest, Hungary
[57] Faculty of Informatics, University of Debrecen, Debrecen, Hungary
[58] HUN-REN ATOMKI – Institute of Nuclear Research, Debrecen, Hungary
[59] Karoly Robert Campus, MATE Institute of Technology, Gyongyos, Hungary
[60] Panjab University, Chandigarh, India
[61] University of Delhi, Delhi, India
[62] Indian Institute of Technology Kanpur, Kanpur, India
[63] Saha Institute of Nuclear Physics, HBNI, Kolkata, India
[64] Indian Institute of Technology Madras, Madras, India
[65] Tata Institute of Fundamental Research-A, Mumbai, India
[66] Tata Institute of Fundamental Research-B, Mumbai, India
[67] National Institute of Science Education and Research, An OCC of Homi Bhabha National Institute, Bhubaneswar, Odisha, India
[68] Indian Institute of Science Education and Research (IISER), Pune, India
[69] Isfahan University of Technology, Isfahan, Iran
[70] Institute for Research in Fundamental Sciences (IPM), Tehran, Iran
[71] University College Dublin, Dublin, Ireland
[72a] INFN Sezione di Bari, Bari, Italy

JHEP05(2026)175

[72b] Università di Bari, Bari, Italy
[72c] Politecnico di Bari, Bari, Italy
[73a] INFN Sezione di Bologna, Bologna, Italy
[73b] Università di Bologna, Bologna, Italy
[74a] INFN Sezione di Catania, Catania, Italy
[74b] Università di Catania, Catania, Italy
[75a] INFN Sezione di Firenze, Firenze, Italy
[75b] Università di Firenze, Firenze, Italy
[76] INFN Laboratori Nazionali di Frascati, Frascati, Italy
[77a] INFN Sezione di Genova, Genova, Italy
[77b] Università di Genova, Genova, Italy
[78a] INFN Sezione di Milano-Bicocca, Milano, Italy
[78b] Università di Milano-Bicocca, Milano, Italy
[79a] INFN Sezione di Napoli, Napoli, Italy
[79b] Università di Napoli 'Federico II', Napoli, Italy
[79c] Università della Basilicata, Potenza, Italy
[79d] Scuola Superiore Meridionale (SSM), Napoli, Italy
[80a] INFN Sezione di Padova, Padova, Italy
[80b] Università di Padova, Padova, Italy
[80c] Universita degli Studi di Cagliari, Cagliari, Italy
[81a] INFN Sezione di Pavia, Pavia, Italy
[81b] Università di Pavia, Pavia, Italy
[82a] INFN Sezione di Perugia, Perugia, Italy
[82b] Università di Perugia, Perugia, Italy
[83a] INFN Sezione di Pisa, Pisa, Italy
[83b] Università di Pisa, Pisa, Italy
[83c] Scuola Normale Superiore di Pisa, Pisa, Italy
[83d] Università di Siena, Siena, Italy
[84a] INFN Sezione di Roma, Roma, Italy
[84b] Sapienza Università di Roma, Roma, Italy
[85a] INFN Sezione di Torino, Torino, Italy
[85b] Università di Torino, Torino, Italy
[85c] Università del Piemonte Orientale, Novara, Italy
[86a] INFN Sezione di Trieste, Trieste, Italy
[86b] Università di Trieste, Trieste, Italy
[87] Kyungpook National University, Daegu, Korea
[88] Department of Mathematics and Physics – GWNU, Gangneung, Korea
[89] Chonnam National University, Institute for Universe and Elementary Particles, Kwangju, Korea
[90] Hanyang University, Seoul, Korea
[91] Korea University, Seoul, Korea
[92] Kyung Hee University, Department of Physics, Seoul, Korea
[93] Sejong University, Seoul, Korea
[94] Seoul National University, Seoul, Korea
[95] University of Seoul, Seoul, Korea
[96] Yonsei University, Department of Physics, Seoul, Korea
[97] Sungkyunkwan University, Suwon, Korea
[98] College of Engineering and Technology, American University of the Middle East (AUM), Dasman, Kuwait
[99] Kuwait University – College of Science – Department of Physics, Safat, Kuwait
[100] Riga Technical University, Riga, Latvia
[101] University of Latvia (LU), Riga, Latvia
[102] Vilnius University, Vilnius, Lithuania
[103] National Centre for Particle Physics, Universiti Malaya, Kuala Lumpur, Malaysia
[104] Universidad de Sonora (UNISON), Hermosillo, Mexico

JHEP05(2026)175

[105] Centro de Investigacion y de Estudios Avanzados del IPN, Mexico City, Mexico
[106] Universidad Iberoamericana, Mexico City, Mexico
[107] Benemerita Universidad Autonoma de Puebla, Puebla, Mexico
[108] University of Montenegro, Podgorica, Montenegro
[109] University of Canterbury, Christchurch, New Zealand
[110] National Centre for Physics, Quaid-I-Azam University, Islamabad, Pakistan
[111] AGH University of Krakow, Krakow, Poland
[112] National Centre for Nuclear Research, Swierk, Poland
[113] Institute of Experimental Physics, Faculty of Physics, University of Warsaw, Warsaw, Poland
[114] Warsaw University of Technology, Warsaw, Poland
[115] Laboratório de Instrumentação e Física Experimental de Partículas, Lisboa, Portugal
[116] Faculty of Physics, University of Belgrade, Belgrade, Serbia
[117] VINCA Institute of Nuclear Sciences, University of Belgrade, Belgrade, Serbia
[118] Centro de Investigaciones Energéticas Medioambientales y Tecnológicas (CIEMAT), Madrid, Spain
[119] Universidad Autónoma de Madrid, Madrid, Spain
[120] Universidad de Oviedo, Instituto Universitario de Ciencias y Tecnologías Espaciales de Asturias (ICTEA), Oviedo, Spain
[121] Instituto de Física de Cantabria (IFCA), CSIC-Universidad de Cantabria, Santander, Spain
[122] University of Colombo, Colombo, Sri Lanka
[123] University of Ruhuna, Department of Physics, Matara, Sri Lanka
[124] CERN, European Organization for Nuclear Research, Geneva, Switzerland
[125] PSI Center for Neutron and Muon Sciences, Villigen, Switzerland
[126] ETH Zurich – Institute for Particle Physics and Astrophysics (IPA), Zurich, Switzerland
[127] Universität Zürich, Zurich, Switzerland
[128] National Central University, Chung-Li, Taiwan
[129] National Taiwan University (NTU), Taipei, Taiwan
[130] High Energy Physics Research Unit, Department of Physics, Faculty of Science, Chulalongkorn University, Bangkok, Thailand
[131] Tunis El Manar University, Tunis, Tunisia
[132] Çukurova University, Physics Department, Science and Art Faculty, Adana, Turkey
[133] Middle East Technical University, Physics Department, Ankara, Turkey
[134] Bogazici University, Istanbul, Turkey
[135] Istanbul Technical University, Istanbul, Turkey
[136] Istanbul University, Istanbul, Turkey
[137] Yildiz Technical University, Istanbul, Turkey
[138] Institute for Scintillation Materials of National Academy of Science of Ukraine, Kharkiv, Ukraine
[139] National Science Centre, Kharkiv Institute of Physics and Technology, Kharkiv, Ukraine
[140] University of Bristol, Bristol, U.K.
[141] Rutherford Appleton Laboratory, Didcot, U.K.
[142] Imperial College, London, U.K.
[143] Brunel University, Uxbridge, U.K.
[144] Baylor University, Waco, Texas, U.S.A.
[145] Catholic University of America, Washington, DC, U.S.A.
[146] The University of Alabama, Tuscaloosa, Alabama, U.S.A.
[147] Boston University, Boston, Massachusetts, U.S.A.
[148] Brown University, Providence, Rhode Island, U.S.A.
[149] University of California, Davis, Davis, California, U.S.A.
[150] University of California, Los Angeles, California, U.S.A.
[151] University of California, Riverside, Riverside, California, U.S.A.
[152] University of California, San Diego, La Jolla, California, U.S.A.
[153] University of California, Santa Barbara – Department of Physics, Santa Barbara, California, U.S.A.
[154] California Institute of Technology, Pasadena, California, U.S.A.
[155] Carnegie Mellon University, Pittsburgh, Pennsylvania, U.S.A.

JHEP05(2026)175

[156] University of Colorado Boulder, Boulder, Colorado, U.S.A.
[157] Cornell University, Ithaca, New York, U.S.A.
[158] Fermi National Accelerator Laboratory, Batavia, Illinois, U.S.A.
[159] University of Florida, Gainesville, Florida, U.S.A.
[160] Florida State University, Tallahassee, Florida, U.S.A.
[161] Florida Institute of Technology, Melbourne, Florida, U.S.A.
[162] University of Illinois Chicago, Chicago, Illinois, U.S.A.
[163] The University of Iowa, Iowa City, Iowa, U.S.A.
[164] Johns Hopkins University, Baltimore, Maryland, U.S.A.
[165] The University of Kansas, Lawrence, Kansas, U.S.A.
[166] Kansas State University, Manhattan, Kansas, U.S.A.
[167] University of Maryland, College Park, Maryland, U.S.A.
[168] Massachusetts Institute of Technology, Cambridge, Massachusetts, U.S.A.
[169] University of Minnesota, Minneapolis, Minnesota, U.S.A.
[170] University of Nebraska-Lincoln, Lincoln, Nebraska, U.S.A.
[171] State University of New York at Buffalo, Buffalo, New York, U.S.A.
[172] Northeastern University, Boston, Massachusetts, U.S.A.
[173] Northwestern University, Evanston, Illinois, U.S.A.
[174] University of Notre Dame, Notre Dame, Indiana, U.S.A.
[175] The Ohio State University, Columbus, Ohio, U.S.A.
[176] Princeton University, Princeton, New Jersey, U.S.A.
[177] University of Puerto Rico, Mayaguez, Puerto Rico, U.S.A.
[178] Purdue University, West Lafayette, Indiana, U.S.A.
[179] Purdue University Northwest, Hammond, Indiana, U.S.A.
[180] Rice University, Houston, Texas, U.S.A.
[181] University of Rochester, Rochester, New York, U.S.A.
[182] Rutgers, The State University of New Jersey, Piscataway, New Jersey, U.S.A.
[183] University of Tennessee, Knoxville, Tennessee, U.S.A.
[184] Texas A&M University, College Station, Texas, U.S.A.
[185] Texas Tech University, Lubbock, Texas, U.S.A.
[186] Vanderbilt University, Nashville, Tennessee, U.S.A.
[187] University of Virginia, Charlottesville, Virginia, U.S.A.
[188] Wayne State University, Detroit, Michigan, U.S.A.
[189] University of Wisconsin – Madison, Madison, Wisconsin, U.S.A.
[190] An institute or international laboratory covered by a cooperation agreement with CERN
[191] An institute formerly covered by a cooperation agreement with CERN

[a] Also at Yerevan State University, Yerevan, Armenia
[b] Also at TU Wien, Vienna, Austria
[c] Also at Ghent University, Ghent, Belgium
[d] Also at Universidade do Estado do Rio de Janeiro, Rio de Janeiro, Brazil
[e] Also at FACAMP – Faculdades de Campinas, Sao Paulo, Brazil
[f] Also at Universidade Estadual de Campinas, Campinas, Brazil
[g] Also at Federal University of Rio Grande do Sul, Porto Alegre, Brazil
[h] Also at University of Chinese Academy of Sciences, Beijing, China
[i] Also at China Center of Advanced Science and Technology, Beijing, China
[j] Also at University of Chinese Academy of Sciences, Beijing, China
[k] Also at China Spallation Neutron Source, Guangdong, China
[l] Now at Henan Normal University, Xinxiang, China
[m] Also at University of Shanghai for Science and Technology, Shanghai, China
[n] Now at The University of Iowa, Iowa City, Iowa, U.S.A.
[o] Also at Helwan University, Cairo, Egypt
[p] Now at Zewail City of Science and Technology, Zewail, Egypt

JHEP05(2026)175

[q] Now at British University in Egypt, Cairo, Egypt
[r] Now at Cairo University, Cairo, Egypt
[s] Also at Purdue University, West Lafayette, Indiana, U.S.A.
[t] Also at Université de Haute Alsace, Mulhouse, France
[u] Also at Istinye University, Istanbul, Turkey
[v] Also at Tbilisi State University, Tbilisi, Georgia
[w] Also at Another institute or international laboratory covered by a cooperation agreement with CERN
[x] Also at The University of the State of Amazonas, Manaus, Brazil
[y] Also at University of Hamburg, Hamburg, Germany
[z] Also at RWTH Aachen University, III. Physikalisches Institut A, Aachen, Germany
[aa] Also at Bergische University Wuppertal (BUW), Wuppertal, Germany
[ab] Also at Brandenburg University of Technology, Cottbus, Germany
[ac] Also at Forschungszentrum Jülich, Juelich, Germany
[ad] Now at RWTH Aachen University, III. Physikalisches Institut A, Aachen, Germany
[ae] Also at CERN, European Organization for Nuclear Research, Geneva, Switzerland
[af] Also at HUN-REN ATOMKI – Institute of Nuclear Research, Debrecen, Hungary
[ag] Now at Universitatea Babes-Bolyai – Facultatea de Fizica, Cluj-Napoca, Romania
[ah] Also at MTA-ELTE Lendület CMS Particle and Nuclear Physics Group, Eötvös Loránd University, Budapest, Hungary
[ai] Also at HUN-REN Wigner Research Centre for Physics, Budapest, Hungary
[aj] Also at Physics Department, Faculty of Science, Assiut University, Assiut, Egypt
[ak] Also at Punjab Agricultural University, Ludhiana, India
[al] Also at University of Visva-Bharati, Santiniketan, India
[am] Also at Indian Institute of Science (IISc), Bangalore, India
[an] Also at Amity University Uttar Pradesh, Noida, India
[ao] Also at UPES – University of Petroleum and Energy Studies, Dehradun, India
[ap] Also at IIT Bhubaneswar, Bhubaneswar, India
[aq] Also at Institute of Physics, Bhubaneswar, India
[ar] Also at University of Hyderabad, Hyderabad, India
[as] Also at Deutsches Elektronen-Synchrotron, Hamburg, Germany
[at] Also at Isfahan University of Technology, Isfahan, Iran
[au] Also at Sharif University of Technology, Tehran, Iran
[av] Also at Department of Physics, University of Science and Technology of Mazandaran, Behshahr, Iran
[aw] Also at Department of Physics, Faculty of Science, Arak University, ARAK, Iran
[ax] Also at Italian National Agency for New Technologies, Energy and Sustainable Economic Development, Bologna, Italy
[ay] Also at Centro Siciliano di Fisica Nucleare e di Struttura Della Materia, Catania, Italy
[az] Also at Università degli Studi Guglielmo Marconi, Roma, Italy
[ba] Also at Scuola Superiore Meridionale, Università di Napoli 'Federico II', Napoli, Italy
[bb] Also at Fermi National Accelerator Laboratory, Batavia, Illinois, U.S.A.
[bc] Also at Lulea University of Technology, Lulea, Sweden
[bd] Also at Consiglio Nazionale delle Ricerche – Istituto Officina dei Materiali, Perugia, Italy
[be] Also at Institut de Physique des 2 Infinis de Lyon (IP2I), Villeurbanne, France
[bf] Also at Department of Applied Physics, Faculty of Science and Technology, Universiti Kebangsaan Malaysia, Bangi, Malaysia
[bg] Also at Consejo Nacional de Ciencia y Tecnología, Mexico City, Mexico
[bh] Also at INFN Sezione di Torino, Università di Torino, Torino, Italy, Università del Piemonte Orientale, Novara, Italy
[bi] Also at Trincomalee Campus, Eastern University, Sri Lanka, Nilaveli, Sri Lanka
[bj] Also at Saegis Campus, Nugegoda, Sri Lanka
[bk] Also at National and Kapodistrian University of Athens, Athens, Greece
[bl] Also at Ecole Polytechnique Fédérale Lausanne, Lausanne, Switzerland
[bm] Also at Universität Zürich, Zurich, Switzerland

JHEP05(2026)175

[bn] Also at Stefan Meyer Institute for Subatomic Physics, Vienna, Austria
[bo] Also at Laboratoire d'Annecy-le-Vieux de Physique des Particules, IN2P3-CNRS, Annecy-le-Vieux, France
[bp] Also at Near East University, Research Center of Experimental Health Science, Mersin, Turkey
[bq] Also at Konya Technical University, Konya, Turkey
[br] Also at Izmir Bakircay University, Izmir, Turkey
[bs] Also at Adiyaman University, Adiyaman, Turkey
[bt] Also at Bozok Universitetesi Rektörlügü, Yozgat, Turkey
[bu] Also at Marmara University, Istanbul, Turkey
[bv] Also at Milli Savunma University, Istanbul, Turkey
[bw] Also at Kafkas University, Kars, Turkey
[bx] Now at Istanbul Okan University, Istanbul, Turkey
[by] Also at Hacettepe University, Ankara, Turkey
[bz] Also at Erzincan Binali Yildirim University, Erzincan, Turkey
[ca] Also at Istanbul University – Cerrahpasa, Faculty of Engineering, Istanbul, Turkey
[cb] Also at Yildiz Technical University, Istanbul, Turkey
[cc] Also at School of Physics and Astronomy, University of Southampton, Southampton, U.K.
[cd] Also at IPPP Durham University, Durham, U.K.
[ce] Also at Monash University, Faculty of Science, Clayton, Australia
[cf] Also at Università di Torino, Torino, Italy
[cg] Also at Bethel University, St. Paul, Minnesota, U.S.A.
[ch] Also at Karamanoğlu Mehmetbey University, Karaman, Turkey
[ci] Also at California Institute of Technology, Pasadena, California, U.S.A.
[cj] Also at United States Naval Academy, Annapolis, Maryland, U.S.A.
[ck] Also at Ain Shams University, Cairo, Egypt
[cl] Also at Bingol University, Bingol, Turkey
[cm] Also at Georgian Technical University, Tbilisi, Georgia
[cn] Also at Sinop University, Sinop, Turkey
[co] Also at Erciyes University, Kayseri, Turkey
[cp] Also at Horia Hulubei National Institute of Physics and Nuclear Engineering (IFIN-HH), Bucharest, Romania
[cq] Now at Another institute formerly covered by a cooperation agreement with CERN
[cr] Also at Another institute formerly covered by a cooperation agreement with CERN
[cs] Also at Texas A&M University at Qatar, Doha, Qatar
[ct] Also at Kyungpook National University, Daegu, Korea
[cu] Also at Yerevan Physics Institute, Yerevan, Armenia
[cv] Also at Imperial College, London, U.K.
[cw] Now at Yerevan Physics Institute, Yerevan, Armenia
[cx] Also at Institute of Nuclear Physics of the Uzbekistan Academy of Sciences, Tashkent, Uzbekistan
[†] Deceased

JHEP05(2026)175